TAMPEREEN TEKNILLINEN YLIOPISTO
TAMPERE UNIVERSITY OF TECHNOLOGY

XIAOCHEN CHEN

DEVELOPMENT AND TESTING OF A WIRELESS STRAIN SENSOR BASED ON ELECTRO-TEXTILE UHF RFID TAGS

Master of Science thesis

Examiner: Postdoctoral Researcher Toni Björninen and prof. Leena Ukkonen
Examiner and topic approved by the Faculty Council of the Faculty of Electrical Engineering
on 23th February 2016

ABSTRACT

XIAOCHEN CHEN: DEVELOPMENT AND TESTING OF A WIRELESS STRAIN SENSOR BASED ON ELECTRO-TEXTILE UHF RFID TAGS
Tampere University of technology
Master of Science Thesis, 54 pages
May 2016
Master's Degree Programme in Electrical Engineering
Major: Wireless Communications Circuits and Systems
Examiner: Postdoctoral Researcher Toni Björninen and Professor Leena Ukkonen
Keywords: UHF RFID, strain sensor tag, antennas, wireless communication

Ultra-High Frequency (UHF) passive RFID tags can be utilized as sensing platforms in the Internet of Things, such as the wireless strain sensor tag. The strain sensor can be used for monitor the human bodily functions and movements.

In my thesis work, the performance and development of a RFID strain sensor was studied to achieve practical usage. This strain sensor is made of a stretchable silver-coated material sewing with no-stretchable coper-coated material, which can stretch 200% of its original length. During the measurement, the elongation of the strain sensor was indicated by the backscattered power of the tag. Thus, the elongation of the sensor can be monitored remotely. However, in the practical environment, the wireless channel is changeable, so the variation of the backscattered power caused by the elongation is the exclusive valuable parameter regardless of the influence of the channel. In this case, the reference tag was introduced to remove the impact of the channel. When two antennas are located closely, it can be considered that they use the same channel to transmit the signal. Thus, a reference tag, which is close to the strain sensor tag, can be applied to characterize the channel features. However, the coupling will affect the performance of the tags unpredictability when two tags are located nearly. My challenge is trying to minimize the coupling effect between the sensor tag and the reference tag.

In this thesis, three different tag configuration models were applied to achieve this goal : the linear configuration, the orthogonal configuration and the parallel configuration. The parallel configuration model performed badly in the chamber test. The backscattered power of reference tag changed a lot with the higher transmitted power at different elongation. As for linear configuration model, the difference of backscattered power between the reference tag and sensor tag (ΔP) was proportional to the sensor elongation, which meant the elongation of the sensor could be read at the reader end approximately. The orthogonal configuration model performed better in both simulation and practical test. Furthermore, the linearity of the elongation and the power difference ΔP is better in this case.

PREFACE

This Master of Science thesis work was carried out in the Wireless Identification and Sensing System Research Group, in the Department of Electronics and Communications Engineering at Tampere University of Technology.

I would like to thanks my supervisor Toni Björninen, who gives me lot of help and inspiration of my thesis work. I really appreciate that I can have the chance to study at WISE group. I have learned a lot in this period.

Tampere, May 2016

Chen Xiaochen

CONTENTS

LIST OF FIGURES

LIST OF SYMBOLS AND ABBREVIATIONS

RFID	Radio Frequency Identification
UHF	Ultra-High Frequency
VHF	Very High Frequency
NLOS	Non-Line-of-Sign
PSD	Power Spectral Density
IC	Integrated Circuit
PIE	Pulse-Interval Encoding
LF	Low Frequency
HF	High Frequency
LO	Local Oscillator
DC	Direct-Current
AC	Alternating-Current
AM	Amplitude-Modulation
HFSS	High Frequency Structure Simulator
PE	Printed Electronics
f	Frequency
T	Period
t	Time
λ	Wavelength
U	Radiation Intensity
P	Total radiated power
Z_a	Impedance of Antenna
e	Radiation Efficiency
Ω_A	Beam Area
ε_M	Beam Efficiency
G	Gain

1. INTRODUCTION

Radio frequency identification, as known as RFID, is a wireless communication technology, which is used for identifying the specific objects or people. It has a wide usage in the physical distribution field and personal identification [1; 2; 3]. A typical RFID system normally consists of three parts: an interrogator (as known as a reader), a transponder (also called tag), and a controller (as known as a host computer). Passive RFID tags are the battery free tags, which have the widest practical usage due to the low cost and small tag size [3]. They communicate with the reader by backscattered power produced by the incident wave transmitted from the reader.

Ultra High Frequency (UHF) passive RFID tags can be utilized as sensing platforms in the Internet of Things [4]. Various sensor RFID tags are widely studied, like temperature sensor tags, gas sensor tags, strain sensor tags, humidity sensor tags, and threshold heat sensor tags, etc. [5; 6; 7; 8]. The strain sensor tag, which is made of conductive and stretchable textile, is studied in this thesis work. This tag can sense the elongation of the attachment, which make them have a wide range of usage, for instance, warning the overlarge movement of patients' limbs, monitoring the chest movement caused by breathing, and monitoring the exercise of athletes to prevent the diseases [9]. The strain sensor system consists of two tags: a sensor tag and a reference tag. By placing the reference tag and the sensor tag closely, it can be considered that the signal utilized between the sensor tag, the reference tag and the reader propagate through the same channel. In this condition, the reference tag is used for indicating the channel characters. Therefore, the reference tag is necessary to maintain a constant respond regardless the sensor stretching [4]. However, when antennas are placed closely, there always has coupling effect between them. It means that while the characters of one antenna is changed, the nearby antenna will be changed corresponding. To reduce the influence from the sensor tag and keep the reference tag work constantly, it is important to minimum the coupling between the nearby antennas by adjusting parameters of this RFID sensor tag system. This thesis is working on achieving this goal.

In this thesis, three different configuration models are designed and tested for reducing the coupling between the reference tag and sensor tag. The measurement results and comparison will be discussed in detail in the following chapters.

The outline of this thesis is described as follow. In Chapter 2, the basics knowledge and background of the antennas are provided. Chapter 3 is a brief introduction to RFID technology. In Chapter 4, the simulation and measurement result are described in detail.

Chapter 5 is the conclusion summarizing all the measurement results in the practical condition.

2. ANTENNAS AND RADIO PROPAGATION

The antenna is a critical component in wireless communication systems, which is used for radiating or receiving electromagnetic waves. It operates as a device, which converts a guided electromagnetic wave (a wave existing in a transmission line) to a plane wave propagating in free space. The one side of an antenna is the voltage source and another side is the air.

2.1 Radiation Mechanism

Radiation is a kind of perturbation in the stable electromagnetic field. The energy always propagates from the source to the free space just like a diffused water wave caused by dropping a stone into a lake. The radiation is caused by the changing current or an acceleration of charge [10].

When an open-end transmission line connects to a source, there is a standing wave, which has a zero current at each half-wavelength point in the line from the end as illustrated in Figure 1. The currents in the two lines have opposite flowing directions as in the picture. Around the transmission lines, there are electric and magnetic field surrounded as shown in Figure 1. The electric field is in the vertical plane of the lines while the magnetic field is encircle the lines. Normally, the wavelength is much greater than the gap between the lines [11].

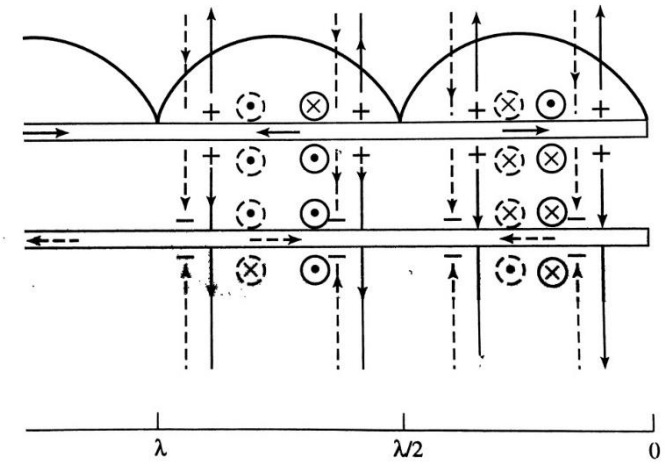

Figure 1. Radiation mechanism [11].

When the end part of the transmission lines change the direction to outwards as in Figure 2, the fields will reveal to the free space. The currents on each vertical line,

whose length is ¼-wave length, have the same flowing direction. In the case of Figure 2, the perturbation is made that transmits outwards.

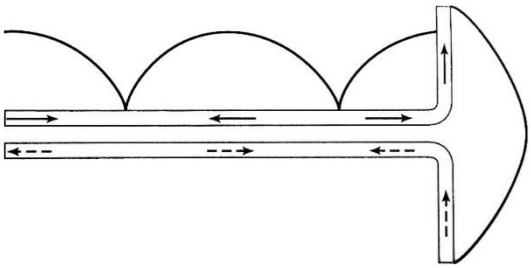

Figure 2. Simple dipole model [11].

The half-wave length dipole connected with an oscillator source (frequency *f*, period $T = 1/f$) and charged separately in Figure 3 [12]. As illustrated in Figure 3, the current caused by the oscillator has flowed ¼ period when $t = 0$. Therefore, the upper part of the dipole is charged by the current and the lower part is deficit charged. In this case, the voltage appears between the two parts of the dipole. The current is created by this voltage from the upper part to lower part. At $t = T/4$, the current reaches the peak charge as shown in Figure 3. and then drops to zero when $t = T/2$. After that, next circulation starts with the negative charge on the upper. The electric field lines will propagate away from the dipole thus the data can be transmitted to the destination then captured by a receive antenna.

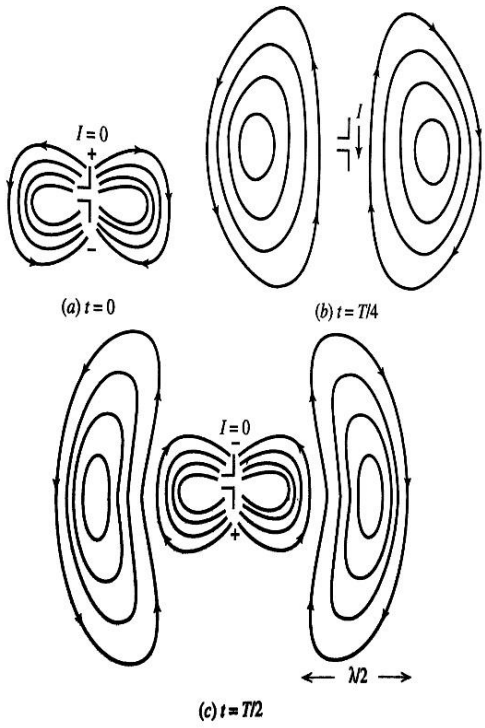

Figure 3. Electric fields of an oscillating dipole for various instants of time [11].

Then, the relations between a collection of sources (the antenna) and the radiated field produced by these sources will be discussed. The antennas can be naturally divided into two types [27]. One is the radiators, such as dipoles, on which the distribution of the current can be predict accurately by a set of formulas. All the far field elements are out of the source volume. The other radiators, such as horns and slots, for which an estimation of the actual current distribution is extremely difficult. However, the close-in field of these antennas can be described quite accurately. There are some far field elements fall into the source volume. The actual sources can be replaced with equivalent sources to do the field calculation. There is an alternate set of formulas used for these cases.

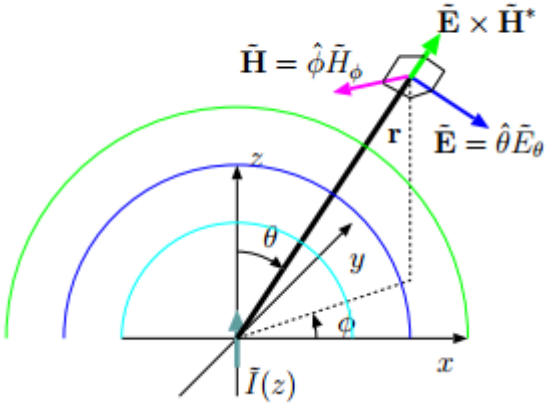

Figure 4. *Radiation field of a short dipole [27].*

The Poynting vector represents the directional energy flux density (the rate of energy transfer per unit area) of an electromagnetic field. The average Poynting vector of radiation fields of the dipole antenna and the "flux" of the same vector can be computed over a sphere imagined to surround the dipole. The Poynting vector **S** can be expressed as:

$$\mathbf{S} \equiv \mathbf{E} \times \mathbf{H}, \tag{2.1}$$

Where **E** is the electric field and **H** is the magnetic field. They are both vector parameters. Thus, the average value of Poynting vector $\boldsymbol{S}_{av}$ can be denoted as:

$$\mathbf{S}_{av} = \frac{1}{T}\int_0^T \mathbf{S}dt = \frac{1}{2}\mathrm{Re}\{\tilde{\mathbf{E}} \times \tilde{\mathbf{H}}^*\} \tag{2.2}$$

Where *T* is the period. Since

$$\tilde{\mathbf{E}} = \hat{\theta}\tilde{E}_\theta, \quad \tilde{\mathbf{H}} = \hat{\phi}\frac{\tilde{E}_\theta}{\eta_0}, \tag{2.3}$$

$$\tilde{E}_\theta = j\eta_0 Ik\ell \sin\theta \frac{e^{-jkr}}{4\pi r}, \tag{2.4}$$

Then we have

$$\mathbf{S}_{av} = \hat{r}\frac{|\tilde{\mathbf{E}}|^2}{2\eta_0} = \frac{\eta_0}{8}|I_0|^2 \frac{|\ell|^2}{(\lambda r)^2}\sin^2\theta\hat{r} \tag{2.5}$$

This expression is the energy flux density where r is the distance, k is the number of waves, θ and ϕ are the angels in spherical coordinates as shown in Figure.4, I is the driving current and $I = I_0 e^{-j\omega t}$, $\ell = \frac{L}{2}$, L is the length of the dipole, λ is the wavelength, η_0 is the intrinsic impedance in free space, around 377 Ohms.

2.2 Antenna Parameters

Antenna parameters have trade-offs between each other. In other words, designers cannot improve an antenna with significant only one parameter of the antenna.

- **Radiation pattern**

Radiation pattern of the antenna refers to the directional dependence of the strength of the radio waves from the antenna or other source. Radiation pattern is used for describing the variation of radiation power in far field, which is always presented in 3-D polar coordinate system [θ, ϕ, δ]. Generally, we only discuss the antenna pattern in the far field because the shape of field pattern is independent of the distance here. The half-power beamwidth (HPBW) or -3 dB beamwidth is the area of the radiation pattern where the radiation power drops to half of the maximum power (or drop -3 dB) [10].

We can also use mathematical formula for present radiation pattern, it is radiation intensity U [watts per unit solid angle]. U can be expressed as:

$$U = r^2 S, \tag{2.6}$$

Where r is the distance from antenna, S is power density which units in [watts per square metre].

First, we consider the condition of an isotropic antenna, which radiated the energy in all the direction equally. If the total radiated power by the antenna is P, so the power density S at one area with r metre from the antenna is:

$$S = \frac{P}{area} = \frac{P}{4\pi r^2}, \tag{2.7}$$

So the radiation intensity can be written as:

$$U = r^2 S = \frac{P}{4\pi}, \tag{2.8}$$

From this formula, we can see that radiation intensity U is very independent of the distance.

Then we consider the case in infinitesimal dipole which is located along the z-axis, the power density is:

$$S_{av} = \frac{1}{2} E_\theta H_\phi^* \hat{r}, \tag{2.9}$$

So the cut of radiation pattern with any value of φ can be expressed as:

$$U = r^2 \times \frac{1}{2} \frac{|E_\theta|^2}{Z_0} = \frac{Z_0}{2} \left(\frac{KI(0)L}{4\pi} \right)^2 \sin^2 \theta, \tag{2.10}$$

Mostly, we express the radiation pattern as normalized:

$$\frac{U}{U_{\max}} = \frac{\frac{Z_0}{2} \left(\frac{KI(0)L}{4\pi} \right)^2 \sin^2 \theta}{\frac{Z_0}{2} \left(\frac{KI(0)L}{4\pi} \right)^2} = \sin^2 \theta, \tag{2.11}$$

At the $\theta = \pi/2$, U has the maximum value [13].

- **Radiation Resistance and Efficiency**

The antenna can be simple expressed as the model in Figure 5:

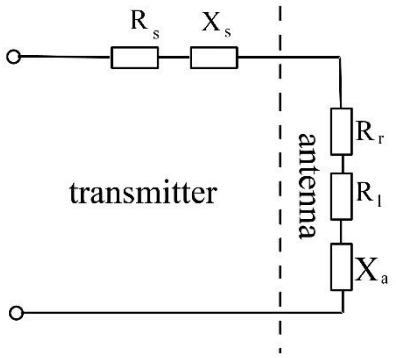

Figure 5. *Antenna's model.*

In antenna part, R_r is radiation resistance, R_l is loss resistance. At R_r some energy radiated out to the air and at R_l some energy lost because of the antenna conductor's resistance [10].

The impedance of an antenna Z_a is defined as:

$$Z_a = R_a + jX_a, \tag{2.12}$$

Where R_a is:

$$R_a = R_l + R_r, \tag{2.13}$$

So the radiation efficiency e can be defined as:

$$e = \frac{\text{Power radiated}}{\text{Power accepted by antenna}} = \frac{R_r}{R_r + R_l}, \tag{2.14}$$

According to the formula, we can see that high radiation efficiency needs small $\frac{R_l}{R_r}$, which means R_r should be larger than R_l.

Impedance matching is the practice of designing the input impedance of an electrical load or the output impedance of its corresponding signal source to maximize the power transfer or minimize signal reflection from the load. To describe the antenna match degree of the resistive source, we use the parameter reflection coefficient ρ :

$$\rho = \frac{V_r}{V_i} = \frac{Z_a - Z_s}{Z_a + Z_s}, \tag{2.15}$$

Where V_r and V_t are the voltage of the reflected wave and incident wave. When $\rho = 1$, $Z_s = 0$ the antenna is totally mismatched means that all the power reflected back and when $\rho = 0$, $Z_a = Z_s$ the antenna is totally matched.

Power transfer efficiency τ is used to measure the quality of the impedance matching between a complex source and a complex load.

$$\tau = \frac{4\mathrm{Re}(Z_a)\mathrm{Re}(Z_s)}{|Z_a + Z_s|^2}, \tag{2.16}$$

When $R_a = R_s$ and $Z_a = Z_s^*$, we can get $\tau = 1$, it means the IC and antenna form a conjugate pair and maximum power is transferred between them.

- **Beam area**

Beam area or beam solid angle is the integral of the normalized radiation pattern over a sphere. The area on the surface of a sphere dA is:

$$dA = (rd\theta)(r\sin\theta d\phi) = r^2 d\Omega, \tag{2.17}$$

Where r is the radius and $d\Omega$ is the solid angle of the area dA. $d\Omega$ is usually unit in steradians [sr] or square degrees [□].

The total area of a sphere is $4\pi r^2$ where 4π is the solid angle of a sphere unit in [sr]. So:

$$1\,\mathrm{sr} = (\text{solid angle of a sphere})/4\pi = 1\mathrm{rad}^2 = \left(\frac{180}{\pi}\right)^2 \deg^2 = 3282.8064\,□,$$

$$4\pi\,\text{steradians} = 41253\,□, \tag{2.18}$$

The beam area Ω_A can be expressed as:

$$\Omega_A = \int_{4\pi}\int P_n(\theta,\phi)d\Omega \quad [\mathrm{sr}], \tag{2.19}$$

Where $d\Omega = \sin\theta d\theta d\phi$ [sr].

The beam area Ω_A can be also expressed by half-power beamwidth approximately:

$$\Omega_A \cong \theta_{HP}\phi_{HP}, \tag{2.20}$$

Where θ_{HP} and ϕ_{HP} are HPBW in two planes [13].

- **Beam Efficiency**

Beam efficiency is the ratio of the transmitted or received power of the main beam and the total transmitted or received power. The beam of an antenna can be divided into two parts: the main beam area and the minor-lobe area:

$$\Omega_A = \Omega_M + \Omega_m, \tag{2.21}$$

So the beam efficiency can be defined as:

$$\varepsilon_M = \frac{\Omega_M}{\Omega_A}, \tag{2.22}$$

Also there has the concept stray factor to describe the ratio between the minor-lobe area and total beam:

$$\varepsilon_m = \frac{\Omega_m}{\Omega_A}, \tag{2.23}$$

And $\varepsilon_M + \varepsilon_m = 1$.

- **Directivity**

The directivity of the antenna can be expressed as a function of directivity D:

$$\begin{aligned} D(\theta,\phi) &= \frac{\text{Radiation intensity of antenna in direction } (\theta,\varphi)}{\text{Mean radiation intensity in all directions}} \\ &= \frac{\text{Radiation intensity of antenna in direction } (\theta,\varphi)}{\text{Radiation intensity of isotropic antenna radiating the same total power}} \end{aligned}, \tag{2.24}$$

So the isotropic antenna has the lowest directivity $D = 1$. All the other antennas have $D > 1$ at the peak directivity in the real environment.

- **Gain**

Antenna gain describes the ability of an antenna converting the incident energy into radio wave or converting the radio wave into the electron power. It is usually defined as the ratio between the radiation intensity of the antenna and the radiation intensity of an isotropic antenna with the same incident energy. The relation between the gain, radiation efficiency and directivity is:

$$G(\theta,\phi) = eD(\theta,\phi), \tag{2.25}$$

- **Polarization**

The electric fields and magnetic fields have x-axis and y-axis components. Therefore, the electromagnetic wave is polarized when it radiates to the air [9]. Polarization is a property of waves that can oscillate with more than one orientation produced by an antenna, evaluated in the far field. There are three different types of polarization: linear polarization, circular polarization and elliptical polarization. The polarization is usually predicated on the characteristic of the electric fields. The electric field has two orthogonal vector components $\boldsymbol{A}$ and $\boldsymbol{B}$. The electric field $\boldsymbol{E}$ can be indicated as:

$$\boldsymbol{E} = \boldsymbol{A}cos\omega t + \boldsymbol{B}cos(\omega t + \beta) \qquad (2.26)$$

$\boldsymbol{A}$, $\boldsymbol{B}$ and $\boldsymbol{E}$ are vector parameters here.

When $\boldsymbol{A} = 0$ or $\boldsymbol{B} = 0$, the wave is linear polarization. The $\boldsymbol{E}$ field vector varies only in one plane as shown in Figure 6 (a) (b).

When $\boldsymbol{A} = \boldsymbol{B}$ and $\beta = -90^{\circ}$, the wave is circular polarization. $\boldsymbol{E}$ field vector varies in two planes with equal magnitude as shown in Figure 6 (c).

When $\boldsymbol{A} \neq \boldsymbol{B}$ and $\beta \neq 0$, the wave is elliptical polarization [14]. $\boldsymbol{E}$ field vector varies in two planes with different magnitude as shown in Figure 6 (d) (e).

Cross polarization is the polarization orthogonal to another polarization. For example, if the E field vector of an antenna is horizontally polarized, the cross polarization of it is vertical polarization.

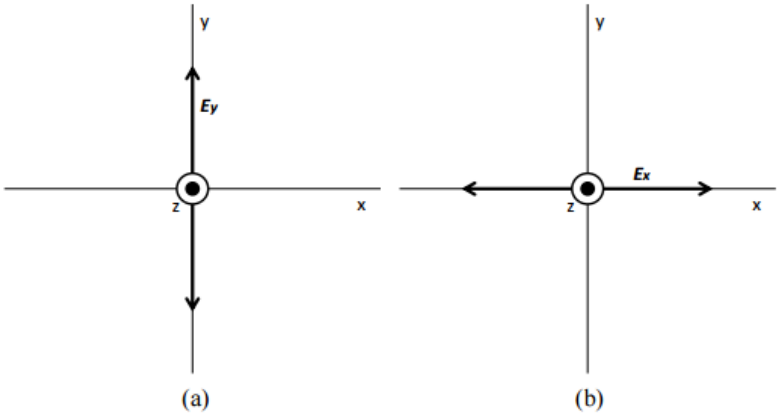

Linear Polarization (a) y-plane (b) x-plane

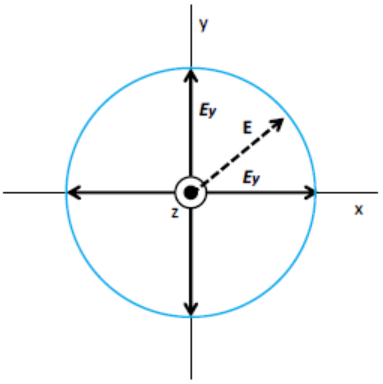

(c) Circular polarization.

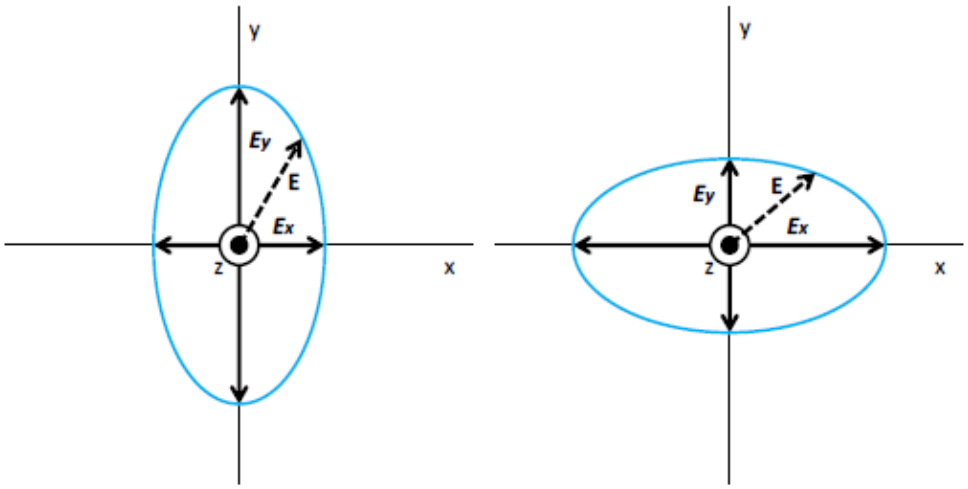

(d) (e)

Elliptical Polarization (d) y-plane (e) x-plane.

Figure 6. *Polarization.*

2.3 Types of Antenna

- **Wire antenna**

The wire antenna is the mostly common antenna which is used everywhere in our daily life. There are many shapes of wire antennas, which we can see on the street, like straight wire, loop wire, and helix wire, which looks like a spring.

Wire antennas are the simplest and oldest antenna with the lowest cost. However, they also have the widest use in practical. Dipole is a kind of typical linear wire antenna, which contains two conduct wires as shown in Figure 7 [15]. Usually the length of the dipole antenna is equal to the half wavelength. In a transmitter or a receiver, the current is flowed into or out of the antenna between the middle of two wires.

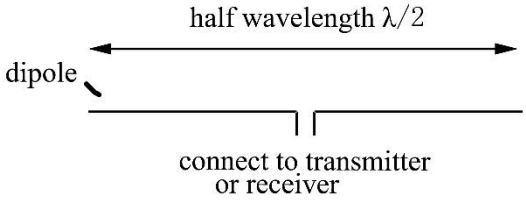

Figure 7. *Dipole.*

The radiated energy of the dipole is equally in all directions so that the radiation pattern of the dipole antenna is omnidirectional as shown in Figure 8.

The loop antenna is another typical kind of the wire antenna which includes a circle wire loop or some other shape of the conductor connected with a balanced transmission line. The circle wire loop antenna is the most common one. The loop antenna can be categorized into two kinds: the small loop (or magnetic loop) antenna and the resonant loop antenna.

The small loop antenna has low radiation resistance which is always smaller than loss resistance and high reactance. The size of small loop antenna is always smaller than one-tenth of the wavelength. Because of these characters, small loop antennas not suit using as a transmission antenna very well. But they can be used as a receiving antenna in some mobile devices.

The resonant loop antenna’s circumference is always equal to the wavelength, which is much bigger than the small loop antenna. So the resonant loop antenna is always used in high frequency band such as Very High Frequency (VHF) 30-300 MHz and Ultra High Frequency (UHF) 300-3000 MHz [16]. Unlike the small loop antenna, the resonant loop antenna has the high radiation efficiency.

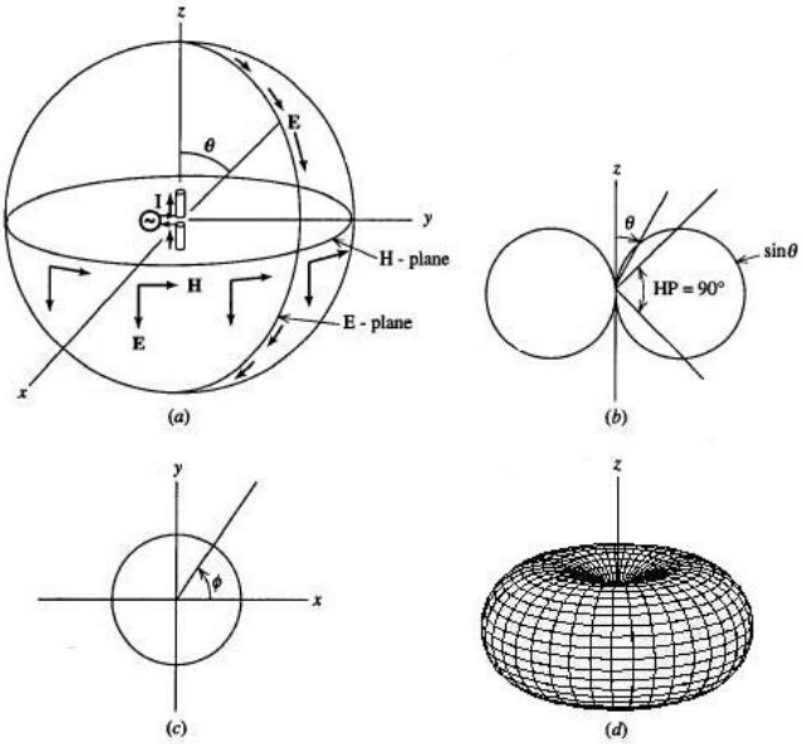

Figure 8. *Radiation pattern of an ideal dipole antenna. (a) Field components. (b) Polar pattern of E - plane. (c) polar pattern of H - plane. (d) 3D plot of radiation pattern [14].*

- **Aperture Antenna**

Aperture antennas are used widely in the microwave field as shown in Figure 9. The aperture antenna usually consists of a waveguide and a horn. The open end used for radiating the power. The aperture antenna typically works as a part in another antenna system like a phase-array antennas and a large reflector antenna. This kind of antenna has some advantages: robustness, wide bandwidth, high aperture efficiency, low VSWR and high polarization purity [17].

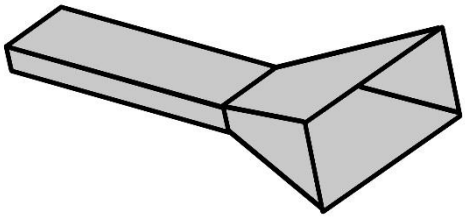

Figure 9*. Aperture antenna.*

The surface of the antenna itself can be covered with a non-conducting material, which is more stable in the outer space environment.

We always analyze the radiation character of the aperture antenna at the far field. So we have formula:

$$E(r) \approx \frac{jk_0 \cos\theta}{2\pi r} e^{-jk_0 r} \mathrm{f}_t\left(k_0 a \cos\theta\cos\phi, k_0 b \sin\theta \sin\phi\right), \quad (2.28)$$

Where r is the distance from the antenna, E(r) is the field strength at the distance r, a and b are the width and length of the wave guide. So from these formulas we can calculate the $E(r)$ if we know the r [18].

- **Microstrip Antenna**

The microstrip antenna, also known as the patch antenna, becomes more and more popular in practical because the shape of the antenna is flat (as shown in Figure 10) and can be achieved by printed electronics (PE). It can be printed on a board directly without using another conductor out of the circuit [19].

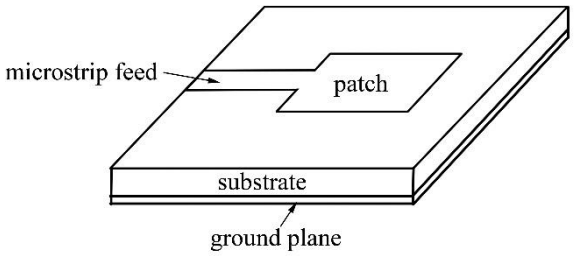

Figure 10. *Path antenna.*

As in Figure 13, the patch antenna consists with a patch, a microstrip feed, a substrate and a ground plane. The power feeds to the patch through the microstrip transmission line when it works as a transmission antenna. The frequency f of the patch antenna depends on the length L of the patch. So the relationship between f and L can be expressed as:

$$f \approx \frac{c}{2L\sqrt{\varepsilon_r}}, \quad (2.29)$$

Where ε_r is the permittivity of the substrate.

The parameters of the patch antenna can be adjusted by adding loads between the patch and the ground plane. Although the patch antenna is very convenient to construct, it also has some limitation like: low antenna efficiency, lower power, narrow bandwidth, and poor polarization purity.

- **Reflector Antenna**

The Reflector antenna, which is often used in the high frequency band, can change the propagation path of the energy by reflecting the electromagnet wave. It consists of a

reflector and a feed antenna. The reflector antenna is a kind of high directivity antenna with the high antenna gain. So it always used in satellite communication which requires high antenna gain. It also used in some secure communication which needs to operate with the narrow beam antennas.

Figure 11. *Parabolic antennas in TUT.*

The parabolic reflector antenna is the simplest reflector antenna consisting with a reflecting dish and a feed antenna on its focal point as shown in Figure 11.The size of the reflector should be bigger than the wavelength and so do the distance between the reflector and the feed antenna [19]. The dish can reflect the wave to the focal point where there is a feed antenna as shown in Figure 12.

Assuming there is a horizontal axis x and a vertical axis y, the dish can be expressed as:

$$x^2 = 4F(F - z), \quad |x| \le \frac{D}{2}, \tag{2.30}$$

Where F is the distance between the focal point and the dish, D is the diameter of the dish.

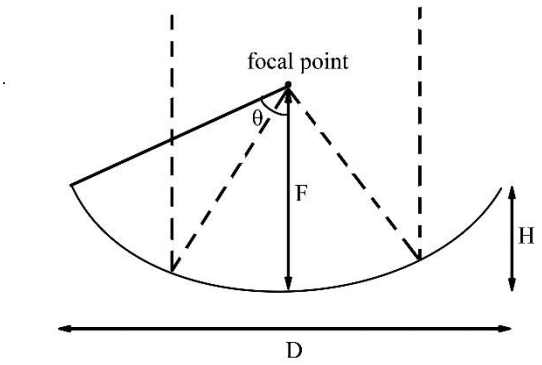

Figure 12. *Parabolic antenna.*

2.4 Propagation Mechanisms

The environment of radio propagation is always complicated and unstable, since when the electromagnetic wave propagates in the air, there are a lot of reflection, scattering and diffraction. The propagation models are the formulas which indicate the relationship between the distance and the power loss in different environments. So they are usually used for predicting the strength of the signals. There are various models which are considered in different conditions, based on the propagation mechanisms we will discuss next.

- Reflection

Reflection happened when the radio wave propagates to the border between two media with different permeabilities and permittivities as shown in Figure 13. When a signal propagates to an obstacle like a wall or ground, some energy will reflects back. If the obstacle is a perfect conductor, the energy will totally reflect back into the first media. But in other case, it will have some loss and phase shift [20].

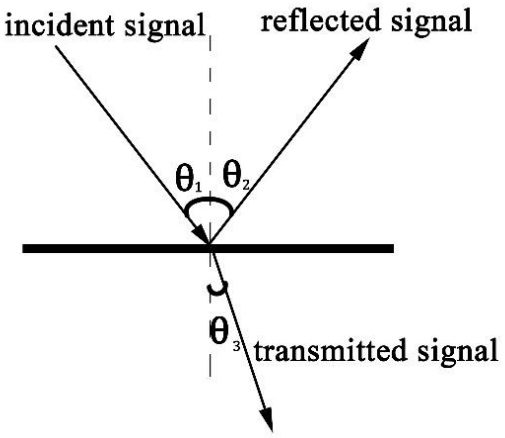

Figure 13. *Signal Reflection.*

And according to Snell's law:

$$\theta_1 = \theta_2 \ , \tag{2.31}$$

The reflection will cause multipath and then make the signal strength changed at the receiver end randomly. Normally, the reflection reduces the signal strength.

- Diffraction

When a radio wave goes through an obstacle or a slit, the phenomenon diffraction will happen. The radio wave will bend when it propagates through the object, which causes the wave falls into the shadow region of the object as shown in Figure 14. When a sharp obstacle locates in front of a light, it will cause a shadow. Due to the diffraction, the edge of the shadow is never completely sharp. This phenomenon can be explained by Huygen's principle [20].

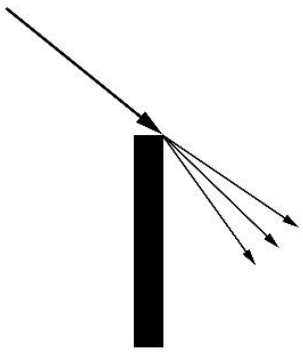

Figure 14. *Diffraction.*

When the radio wave goes through the bordering of the obstacle such as buildings or trees, diffraction will happen. The wave falls into the shadow region with a non-line-of sign (NLOS) path, which will change the path of the wave propagation though the signal can still be received by users. The diffraction depends on the parameters of the signal like phase, amplitude and polarization. The loss caused by diffraction is much higher than the reflection.

- Scattering

When the wave propagates to a rough surface, the reflection wave may back into many different directions simultaneous as shown in Figure 15. This phenomenon is called scattering. When the surface is rougher, the reflected wave scatters to more directions and broadens more of the energy. Scattering attenuate the signal from the incident direction but increase the reflected signal to other directions. The direction of reflected signal

which caused by scattering depends on the incident angle and the ratio of the roughness and the wavelength [20].

The strength of the scattering wave is always weaker than the incident wave because the energy is scattered to many different directions.

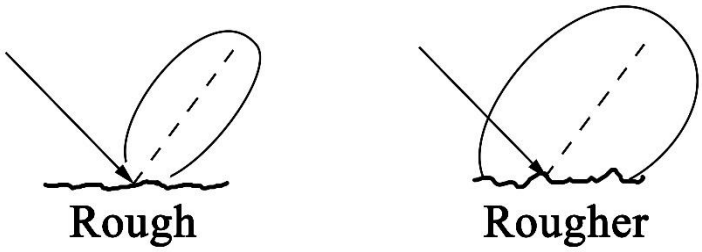

Figure 15. *Scattering.*

2.5 Multipath Propagation

In wireless communication, the signal transmits between transmitters and receivers via channels. Signals can use many different paths to reach the receiver from the transmitter by reflection, diffraction and scattering or the combination of them. Of course, the signal can also propagate by line-of-sign path from transmitter to receiver. The multipath propagation is illustrated in Figure 17. The signal of the different path may have the change in amplitude, phase and angles at the receiver and they may cause interference to each other.

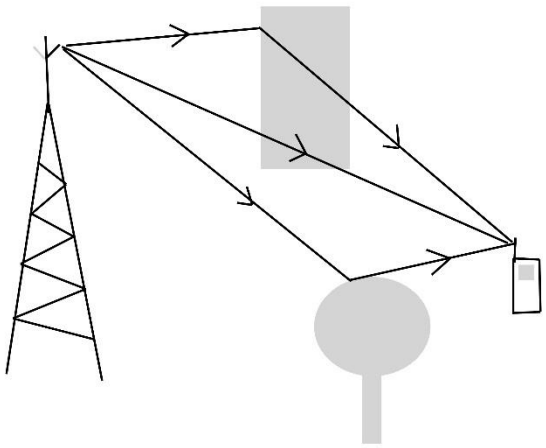

Figure 16. *Multipath.*

- **Coherence Time**

Coherence time T_{coh} is the maximum time different between two signals' paths which arrive at the receiver end in the same channel. In other words, if the time different between two transmitted signals is less than T_{coh}, we consider they propagate in the same

channel. In practice, we use "50% coherence time" definition more usual. It means that we measure 0.5 T_{coh} or more [21].

The nominal width of the Doppler power spectral density (PSD), B_d, is the Doppler spread. The coherence time T_{coh} is inversely proportional to the Doppler spread of the channel:

$$T_{coh} \sim \frac{1}{B_d}, \tag{2.32}$$

- **Coherence Bandwidth**

Coherence bandwidth B_{coh} is the maximum bandwidth of a channel which can be assumed to be approximately constant in frequency within this bandwidth. It means that if the bandwidth of a signal is less than the coherence bandwidth, this signal will be affected by this channel. The frequency components in a bandwidth of a signal are greater than the B_{coh} are distorted in an uncorrelated manner. A channel is considered as a wideband when signal bandwidth is bigger than coherence bandwidth and a narrowband when signal bandwidth is smaller than coherence bandwidth. The fading type of a signal depends on the relation between the coherence bandwidth and signal bandwidth. If the coherence bandwidth is smaller than signal bandwidth, it will have frequency selective fading and if the coherence bandwidth is bigger than signal bandwidth it will have flat fading [21].

The relationship between coherence bandwidth B_{coh} is inversely proportional to multipath caused delay spread:

$$B_{coh} \sim \frac{1}{T_m}, \tag{2.33}$$

2.6 Fading

With a constant transmit power, the signal power level at the receiver end can be different because of the fading. We can categorize fading into large-scale fading and small-scale fading, or fast fading and slow fading [22]. The relationship between then can be read in Figure 17.

- **Slow Fading**

Slow fading is also named large-scale fading, shadow fading or long-term fading. It caused by the shadow of buildings, walls or trees, which can reduce or even block the signal strength. The radio signal can propagate through the shadow by reflection, dif-

fraction or/and scattering. The variation of the mean signal level at a receiver, which is the mean value of fast fading, is called slow fading [22].

- **Fast Fading**

Fast fading is also named small-scale fading, multipath fading or short-term fading. It is the rapid change of signal amplitude in a short time or travel distance at the receiver while the slow fading is always not changed amplitude as such significant. The reflecting path and scatter can create a constantly changing multipath model. A radio signal propagates from transmitter to receiver via different paths may have different delay and then they add up at the receiver end constructively or destructively. The prediction of accuracy signal strength in multipath environment is also hard because of lacking of the knowledge of all signal path.

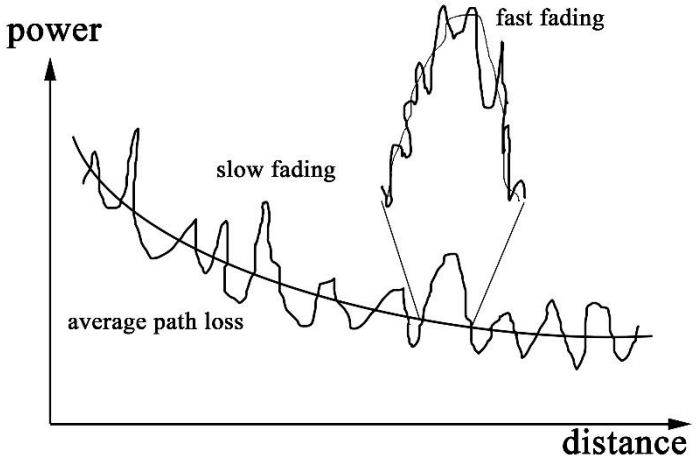

Figure 17. *Fading.*

3. RFID TECHNOLOGY

3.1 Introduction to RFID system

Radio frequency identification, as known as RFID, is a wireless communication technology, which is used for identifying the specific objects or people [23]. It has a wide usage such as:

- Tracking the cargoes which being used by the major retail chains of Wal-Mart, K-Mart and other similar companies.
- Access control. By identifying the ID card of the employees, the RFID system can achieve the access control.
- Animal tracking, which has been used for a long time in breeding industry and now start to use on pets.
- Automatic toll collection. RFID can identify the passing by vehicles and charge them automatically.
- Vehicle tracking and security system.

A typical RFID system usually consists of an interrogator, as known as a reader, a transponder, also called tag, and a controller which is always a host computer. There are antennas attached to both the reader and the tag, which used for converting the voltages to the electromagnetic waves and vice versa as shown in Figure 18 [3].

The tag has an integrated circuit (IC), which is used for storing the identification information and transmitting the data to the reader, and the reader usually connects to a host computer to concern with the data. The host computer can be operated by users to control the reader and store or display the information on its scream.

RFID tags can be categorized into three different types: active tags, semi-passive tags and passive tags [2].

Active tags integrate a battery as a power source. When they are working, they use their own battery to achieve the transmission to the interrogator. In this case, active tags can communicate with the reader within a long range up to several kilometers, large memories and suffer from less interference. However, there are also some shortages of the active tag such as high cost, large tag size and the limited life time (two to seven years) of the battery [3].

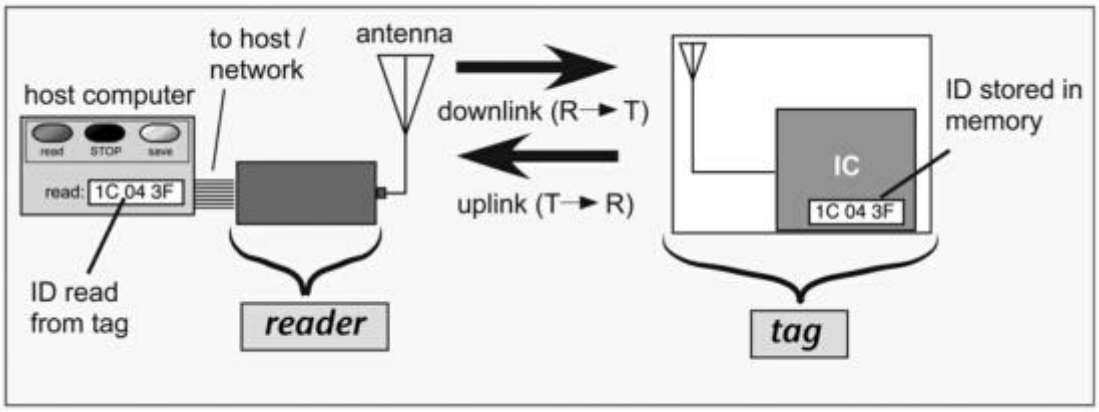

Figure 18. *RFID system [2].*

Semi-passive tags also have the battery on-board and get the energy form the interrogator at the same time. The local battery powers the integrate circuit of the tag. As for the data transmission, semi-passive tags use backscattered communication to send the information. The read ranges of semi-passive tags are from 10 to 100 meters. They suffer from the same problems with active tags.

Passive tags don't have the independent power source or the radio transmitter on-board. Instead, they utilize the received power from the reader to transmit the data, which is much less than the power supported by the battery. When the interrogator sends a signal to the passive tags, they catch the energy of the signal then backscatter the data to the reader. In this case, passive tags are always smaller and cheaper. However, the valid read ranges of passive tags are smaller than active tags. Thus, passive RFID tags have the widest practical usage.

3.2 The working principle of RFID systems

Similar to wireless communication systems of the other kind, readers and tags of RFID system also communicate with each other via electromagnetic waves. In order to generate the continued signal, the voltage of the signal should be a periodic function with the period T, and frequency f which is equal to $1/T$.

To transmit the information, waves should be modulated to carry the data. Because the uninterrupted power is mandatory for passive RFID tags, the coding approach pulse-interval encoding (PIE) is used for RFID. PIE uses a short power-off pulse following a long power interval to express the binary "1", and a shorter full-power interval with the same power-off pulse to indicate the binary "0" as shown in Figure 19.

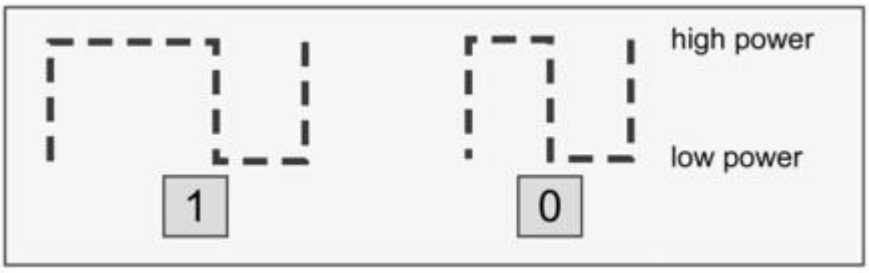

Figure 19. *Pulse-interval coding baseband symbols [2].*

Passive tags use the modulation reflected power which received by the tag antenna since they don't use the on-broad battery to support the transmission. The principle of backscatter radio links is shown in Figure 20. The transmit antenna send initial waves to the receive antenna. At the receive antenna end, the current flow will be generated if the impediment is small. The current flow in the receive antenna should be the same with the transmit antenna and can lead the radiation wave, backscattered signal, which can be detected by the transmit antenna.

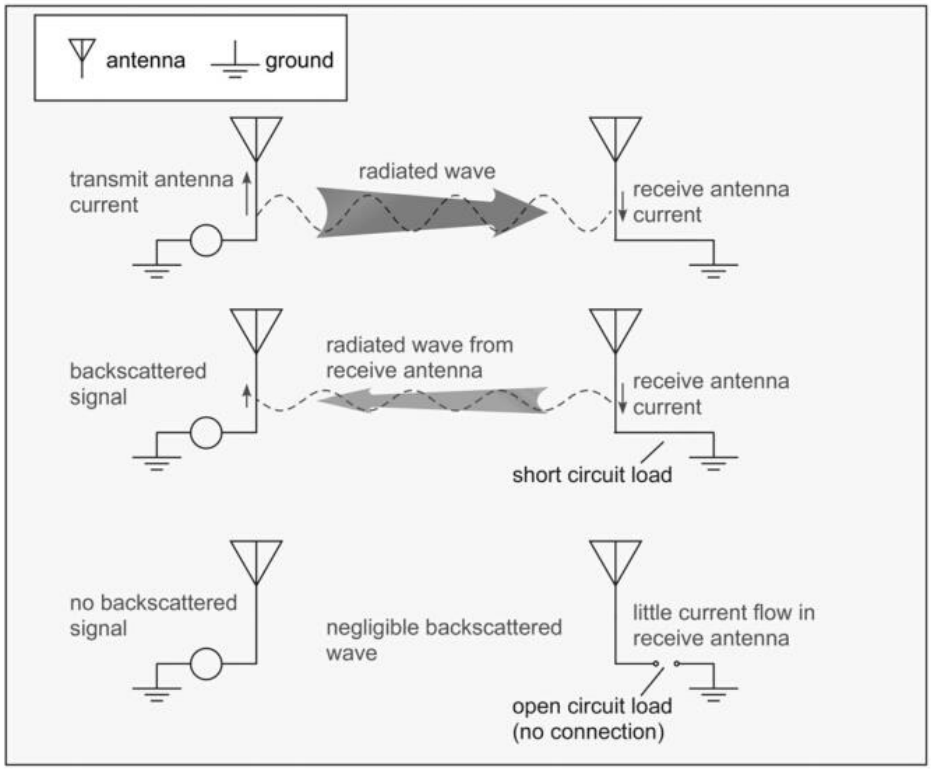

Figure 20. *Backscatter modulation [2].*

To maintain the connection between the reader and the tag, the minimum power level which can ensure the data transmission successfully by tags should be known. RFID designers can set the parameters of the system by calculating the link budget. When the reader and the tag communicate mutually, there are two separate link budgets, from the reader to the tag and vice versa.

The polarization of the radiated wave is also a significant part which should be taken into account when building a RFID system. If the polarization of the radiated waves transmitted from the reader is unmatched with the tag antenna, the received power will be reduced. This may lead the tag cannot be active by the received power.

3.3 Operation frequency bands

RFID systems are a kind of radio systems which communicate via electromagnetic waves [1]. The frequencies utilized by RFID are from 100 kHz to 5 GHz as shown in Figure 21. It is vitally importance to ensure that there is no interference signal which can affect the RFID systems around the RFID devices. To achieve this, RFID systems usually only possible to use several specific frequency bands that be reserved for the particular cases.

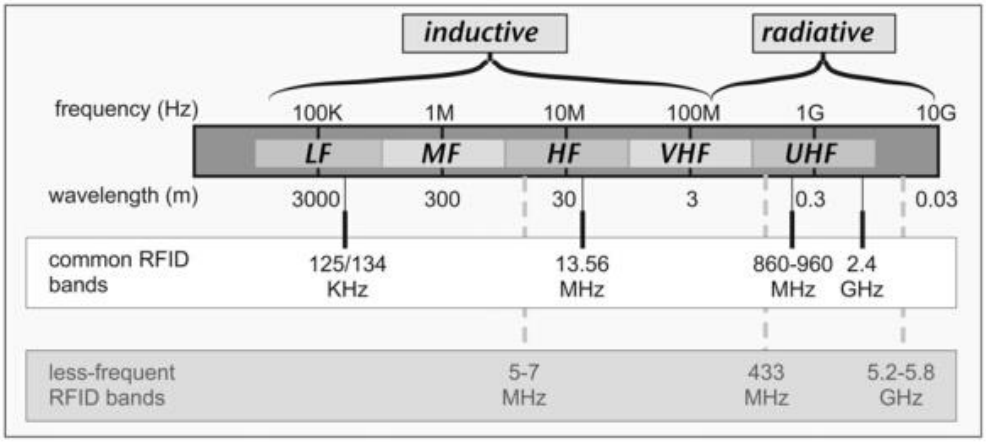

Figure 21. *RFID frequency band [2].*

The most commonly utilized RFID frequency bands are 125/134 kHz, 13.56 MHz, 860 – 960 MHz and 2.4 – 2.45 GHz. The RFID systems using 125/134 kHz bands, which is within low frequency (LF) band, referred to LF systems. 13.56 MHz working frequency band is high frequency (HF) band. The systems, which work in this band, are HF systems. The systems operate 900 MHz and 2.4 GHz are within ultra-high-frequency (UHF) band. The operating frequency bands of different countries are shown in Table 1. The microwave band 2.4 GHz – 2.45 GHz is unlicensed, which used in industrial, medical and scientific radio band.

The wavelength (λ) depends on the frequency (*f*). The travelling speed of electromagnetic waves is the speed of light, c = 300000000 meters per second (m/s). The relation between the wavelength, light speed and frequency is:

$$\lambda = \frac{c}{f}, \tag{3.1}$$

Thus, the wavelength of RFID systems is common from 2000 m to 12 cm. Because of the limitation of the area, the antenna sizes of RFID are usually from 0.01 m to 1 m. Therefore, in LF and HF systems, the wavelength is much larger than the antenna size. They are typically inductively coupled between the readers and tags. In this case, almost all the transmitted energy is around the reader antenna and dropping down quickly as the distance. In UHF systems and microwave systems, which the antenna sizes are comparable to the wavelength, usually employ radiative coupling. The tags can be read in the far field of the readers. Thus, comparing with the inductively coupled, radiative coupling has a larger read range.

Table 1. *UHF frequency regulations.*

Region	Frequency band [MHz]
Europe	865.6 – 867.6
United State, Canada	902 - 928
China	920.5 – 924.5

3.4 Passive UHF RFID system

3.4.1 UHF RFID Readers

In a passive UHF RFID system, the reader needs to be both the transmitter and the receiver, which works on sending the signal to the tag and reading the backscattered information. There are some basic requirements of the RFID system such as accuracy, efficiency and accuracy. The key components of RFID reader construction are shown in Figure 22.

The bistatic antenna is necessary for the RFID reader to works as both the transmit antenna and the receive antenna. It utilizes to convert the voltage to the electromagnetic waves and vice versa. The position of the antenna should be located, where the reader zone can cover all the possible place of tags.

The amplifier is used for increasing the power level, in other words, it introduces a power gain into the system. The useful signal which caught by the antenna may be small, for instance -60 dBm, which cannot be converted conveniently. Thus, the amplifier is significant for digitizing the received analog signal.

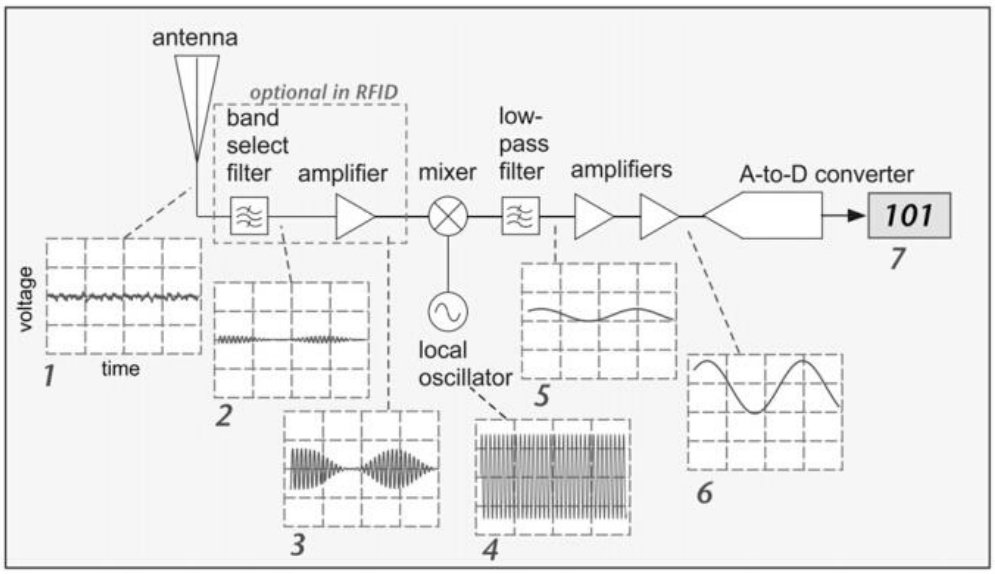

Figure 22. *Components of a RFID reader when it works as a receiver [2].*

The function of a mixer is to move a signal from one frequency to another with protecting the modulated information not being destroyed. This purpose can be realized by the local oscillator (LO) signal which has the constant phase and amplitude. The local oscillator generates a signal, which has the same frequency with the carrier but the inverted phase. When the LO signal and the modulated signal go through the mixer, the output is just some modulated information without the carrier.

Filters can remove some noise of the signal. They often work with mixers and the LO signal to pass the target signal and block the others.

All the RFID readers use the digital signal to carry the information and then convert it into the analog signal to transmit. When they work as a receiver, they convert the received analog signal to digital data for decoding and interpretation as well. Because of the limitation of passive tags, a simple digital-analog converter is needed in the RFID reader systems.

3.4.2 Passive UHF RFID Tags

RFID tags are always attached to the objects, which needed to be identified or tracked and normally more expansive than tags. Passive RFID tags essentially consist of the antenna and the integrate circuit as shown in Figure 23.

Passive RFID tags acquire the power from the incident signal, which comes from the reader. Tags send the information by backscatter modulation. There is a balance of the amount between the backscattered power and the retained power, which can be obtained by changing the capacitance on tags. Figure 23 shows the elements of a passive UHF tag. To operate a passive RFID tag, the IC needs direct-current (DC) power which is a

constant voltage source. The level of the power is around 1 to 3 volts depending on the circuits. This source is get from the incident RF signal around 900 MHz and backscattered to the reader with 0.1 – 0.3 volts magnitude.

First, the tags use a diode to change the alternating (AC) voltages to DC voltages. Diode only allowed current flowing in one direction. The received power is less than then the working power of IC so a charge pump is needed to contain and increase the power level for IC. Since the signal comes from the reader is the amplitude-modulated (AM) signal, the IC need to demodulate the signal by generating a baseband voltage whose magnitude is proportional to the peak voltage of the reader signal. Then IC simply interrupts current flow through the antenna to modulate the scattered power and reply to the reader.

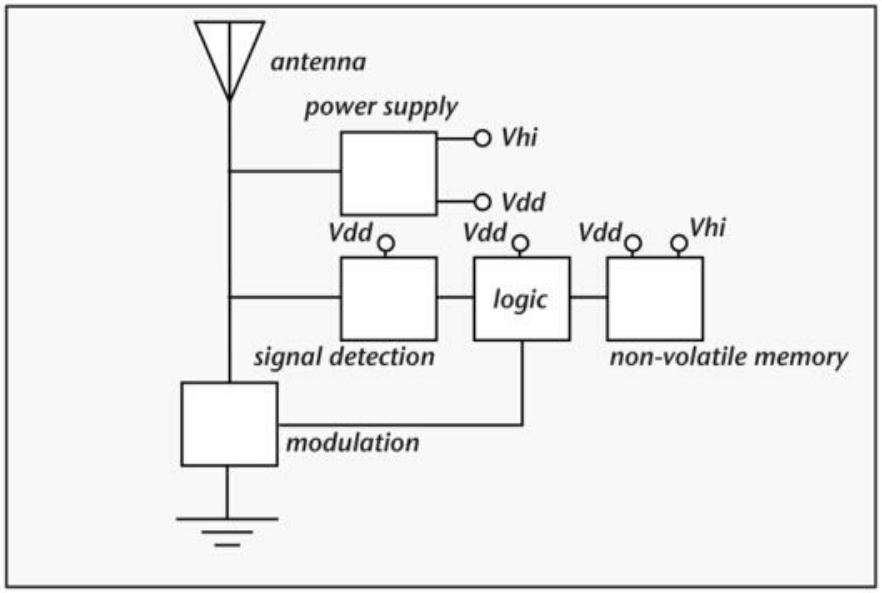

Figure 23. *Elements of a passive UHF tag [2].*

Low cost and marginal power are the two main challenges of RFID tags' designing. The cost of a chip always depends on the size, which can be reduced by scaling. Scaling is the way to minimizing the chip size with the fix number of the transistors by reduce the size of transistors due to improvements in lithography and processing.

3.5 RFID Sensor Tags

The read ranges of UHF RFID tags can reach 25 meters by utilizing a specific mechanism of digital modulation scattering without any on-board batteries [4]. Thus, the passive RFID tags can work in the Internet of Things as sensing platforms or digital devices. Various sensor RFID tags are widely studied on this occasion, like temperature sensor tags, gas sensor tag, humidity sensor tags, threshold heat sensor tags, etc.

In my thesis work, I study the strain sensor tags, which can sense the elongation of the attachment, using conductive and stretchable textile. The backscattered power strength changed linearly with the elongation thus we can notify the strain and read the stretch through the different backscattered power. The strain sensor tags can be utilized for healthcare such as warning the overlarge movement of patients' limbs, monitoring the chest movement caused by breathing. In addition, strain sensors can also monitor the exercise of athletes to prevent the diseases [9]. The tags are made of two different metallized fabrics sewing together by metal-coated thread [4]. These novel fabrics materials are well-conductive and light in weight.

4. EXPERIMENT

4.1 Tools

- High Frequency Structure Simulator

High Frequency Structure Simulator (HFSS) is the first commercial finite element method simulation software for electromagnetic from the company Ansys, which is one of the most popular simulation softwares and an essential tool for engineers [25]. HFSS is used for analysis antennas, as well as design of other RF circuit components such as filters, packaging and transmission lines [24]. Concise operation interface and accurate self-adapting field solver are the most significant features of HFSS. It has the ability to calculate antenna parameters such as antenna gain, directivity, radiation pattern, HPBW, efficiency.

- Tagformance

Tagformance is used to do the measurement for evaluating the performance of RFID systems. This system has three parts: Tagformance lite measurement device, software package and accessories as shown in Figure 24. The main functions of Tagformance are:

- Measure tag sensitivity
- Tag behaviour analysing
- Study forward and return like balance and system level read range
- Realize the environmental interferences
- Test or verify tag protocol

Tagformance can be utilized in tag design, RFID deployment, RFID tag testing and analysis, tag quality monitoring, protocol testing and academic researching [31].

Figure 24. *Tagformance device.*

4.2 Simulation

In my study, the T-matched dipole is used to make the sensor tag antenna. The elongation of the strain is indicated by the backscattered power of the tag. We want the variation of the backscattered power only caused by the stretch of the sensor, so the influence caused by the channel need to be removed. By putting two antennas closely it can be considered that they use the same channel to transmit the signal. Thus, I put a reference tag closely to the sensor tag to characterize the channel features. But there comes a problem, when two antennas located nearly, they will have coupling effect between each other. It means when an antenna changes its characters, the other antenna will change correspondingly. My challenge is trying to minimum the coupling effect between tags.

According to the previous work, the shape of the textile antenna we choose is shown in Figure 25 [26]. For sensor tag, the unstretchable part, as well as the main body of the textile antenna, is made of a highly conductive copper fabric (Less EMF Pure Copper Polyester Taffeta Fabric Cat. #A1212). The stretchable silver-coated fabric (Less EMF Stretch Conductive Fabric Cat. #321) is sewed with the copper fabric to make the stretchable part of the antenna. The stretchable material can strain to 200% of the original length. The length of stretchable part is 30 mm thus the maximum strain length is 30 mm. For the reference tag, the copper fabric is utilized to make the whole antenna. The tag IC we choose to use is NXP UCODE G2iL series RFID IC with the wake up power of -18 dBm.

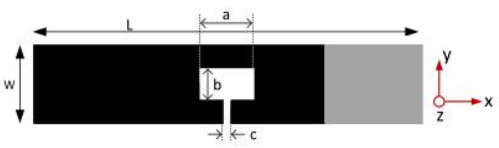

Figure 25. *The shape of the tag antenna.*

The size and configuration of the tags are what we need to design to minimum the coupling between them. In HFSS simulation, we observe the read range calculating from the simulated parameters to see the influence caused by coupling.

The read ranges of passive RFID tags depends on the forward link from reader to tags. In free space, the read range of the tag is [4]:

$$d_{tag}(\phi,\theta)=\frac{\lambda}{4\pi}\sqrt{\frac{\chi_{pol}(\phi,\theta)\tau e_r D(\phi,\theta)EIRP}{P_{ic0}}}, \tag{4.1}$$

$$\tau=\frac{4\mathrm{Re}(Z_a)\mathrm{Re}(Z_{ic})}{|Z_a+Z_{ic}|^2}, \tag{4.2}$$

Where λ is the wavelength of the signal, EIRP is the isotropic transmitted power of the reader, P_{ic0} is the IC wake up power, χ_{pol} is the polarization power efficiency between the tag antenna and reader antenna, which is assumed 1 here, e_r is the antenna radiation efficiency of the tag, D is antenna directivity, τ is the IC-antenna power transfer efficiency depending on the impedances of IC and antenna. In Europe, the EIRP of RFID is 3.28 W.

The system, which contains a sensor tag and a reference tag, can be considered as a two port system. In two port system, the impedance of the antenna and tag IC cannot be measured directly. So the formula is used to calculate the impedance [28]:

$$Z_{in}=Z_{11}-\frac{Z_{12}Z_{21}}{Z_{22}+Z_{ic}}, \tag{4.3}$$

$$Z_{out}=Z_{22}-\frac{Z_{12}Z_{21}}{Z_{11}+Z_{ic}}, \tag{4.4}$$

$$\tau_{in}=\frac{4\mathrm{Re}(Z_{in})\mathrm{Re}(Z_{ic})}{|Z_{in}+Z_{ic}|^2}, \tag{4.5}$$

$$\tau_{out}=\frac{4\mathrm{Re}(Z_{out})\mathrm{Re}(Z_{ic})}{|Z_{out}+Z_{ic}|^2}, \tag{4.6}$$

Where

$$Z_{11}=\frac{V_1}{I_1}, \quad I_2=0, \tag{4.7}$$

$$Z_{12}=\frac{V_1}{I_2}, \quad I_1=0, \tag{4.8}$$

$$Z_{21} = \frac{V_2}{I_1}, \quad I_2 = 0, \tag{4.9}$$

$$Z_{22} = \frac{V_2}{I_2}, \quad I_2 = 0, \tag{4.10}$$

V and *I* are the voltage and current at the ports.

The two antenna ICs can be considered as a input port 1 and a output port 2. The impedance of the input port is Z_{in}, output port is Z_{out}. Thus we can calculate the read range of sensor tag and reference tag separately by using τ_{in} and τ_{out}.

The backscattered power at the reader end is [4]:

$$P_{rx} = \frac{1}{4}|\rho_1 - \rho_2|^2 \left(\frac{\lambda}{4\pi d}\right)^4 G^2 G_{read}^2 P_{tx}, \tag{4.11}$$

$$\rho_k = \frac{Z_{ic,k} - Z_a^*}{Z_{ic,k} + Z_a}; \quad k = 1,2, \tag{4.12}$$

Where *d* is the distance between tag antenna and reader antenna, P_{tx} is the transmitted power of the reader, G and G_{read} are the antenna gain of the tag antenna and reader antenna, ρ_1 and ρ_2 indicate the power reflection coefficient.

From the equation (4.7), we can see that P_{rx} is proportional to the square of tag antenna gain, G^2. Thus, if we need the constant P_{rx} of the reference tag, the G^2 of the tag antenna should be stable. In order to read the strain, the G^2 of the sensor should change linearly with the elongation as well.

In my simulation, HFSS measures the parameters of the antenna at the threshold working power of the IC. There are three goals I should achieve in simulation: The read range of the stretchable tag should be around 8m when it stretched. The read range of the reference tag should be higher than the stretchable tag. The square of the antenna gain of the stretchable tag should be proportional to the stretched length. For reference tag, it should be stable.

First I utilize the parallel configuration of the tag antennas as shown in Figure 26. to minimize the coupling between tags. The size of the antennas, the size of the matching slots, distance between the sensor tag and the reference tag and the orientation of the IC can be adjusted to optimize the simulation result. My target frequency band is 865.6 MHz ~ 867.6 MHz. The simulation result is shown in Figure 26.

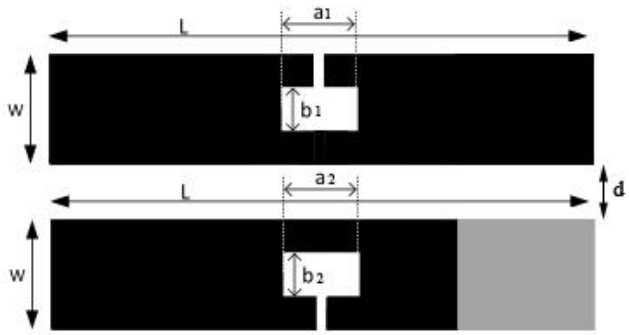

a1	b1	a2	b2	L	W	d
18.7mm	10mm	18.6mm	9.73mm	100mm	20m	10m

(a) The parallel configuration

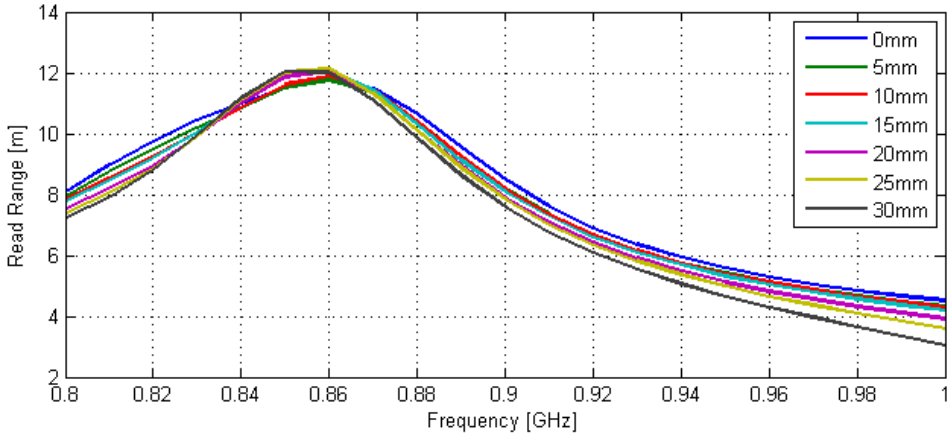

(b) Read ranges of the reference tag

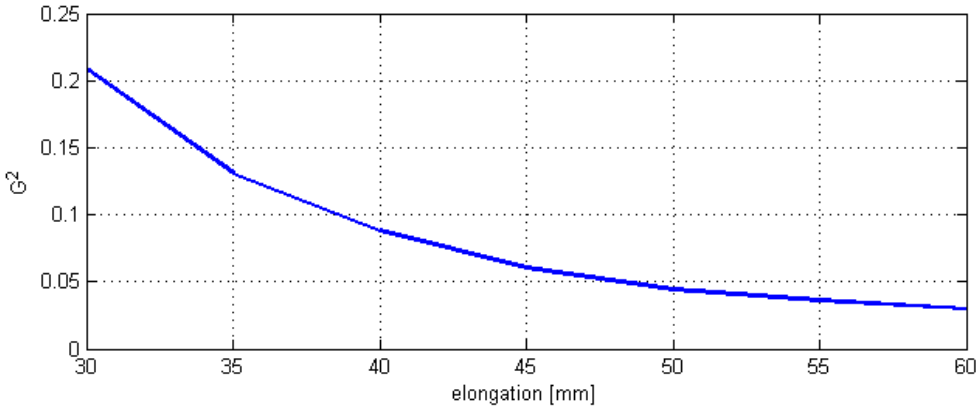

(c) G^2 of the reference tag

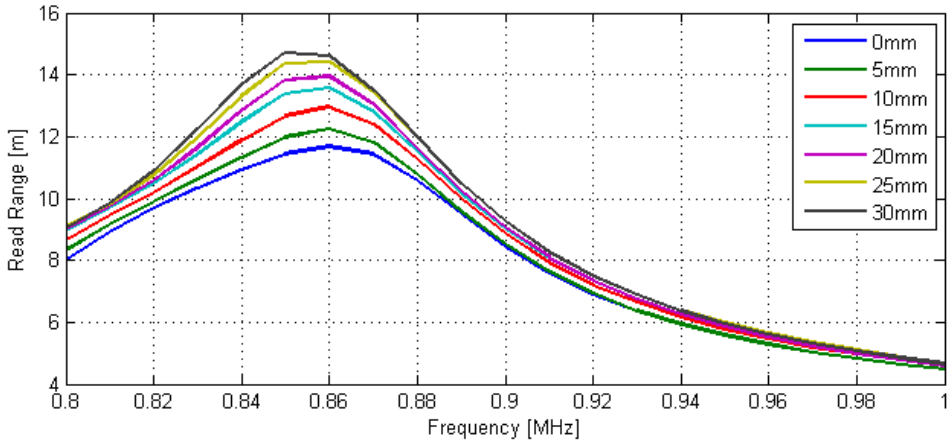

(d)Read ranges of sensor tag

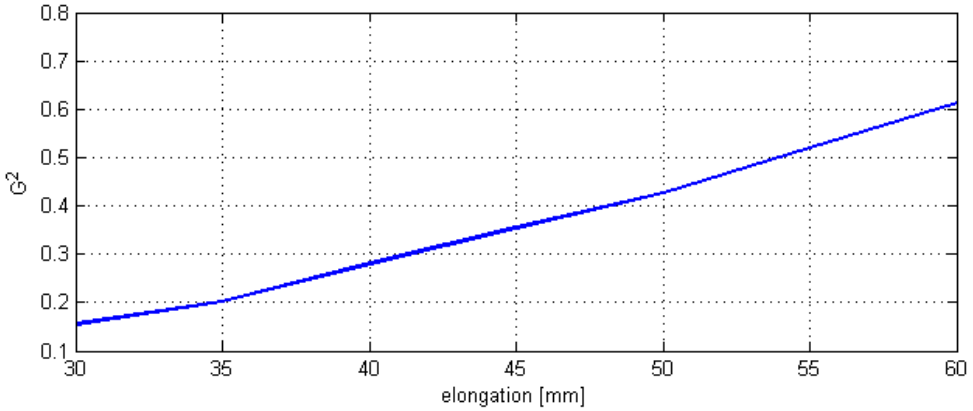

(e) G^2 of sensor tag

Figure 26. *The simulation result of parallel configuration model.*

The read rang of the reference tag is around 11.6 m at target band. The maximum variation of G^2 is 0.1, thus it can be considered stable with the strain of the sensor. For the sensor tag, the read ranges are from 8.5 m ~ 11.5 m, which are lower than the reference tag. For the sensor tag, G^2 is also linear with the elongation.

The second model utilizes linear configuration, the size parameters and configuration are illustrated in Figure 27. The distance between the sensor and the reference tag is 10 mm. The ports of the sensor tag and the reference tag are on different sides. When the sensor stretching, the distance between the tags is keeping constant and outwards part of the sensor is stretching.

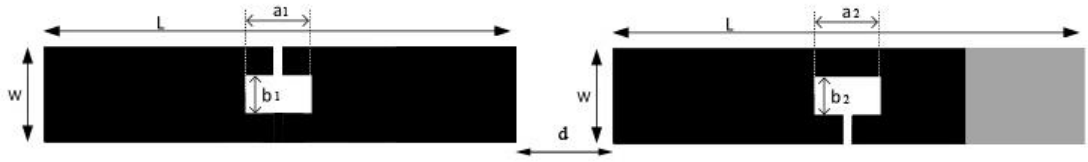

a1	b1	a2	b2	L	W	d
18.7mm	10mm	18.6mm	9.73mm	100mm	20m	20m

(a) The linear configuration

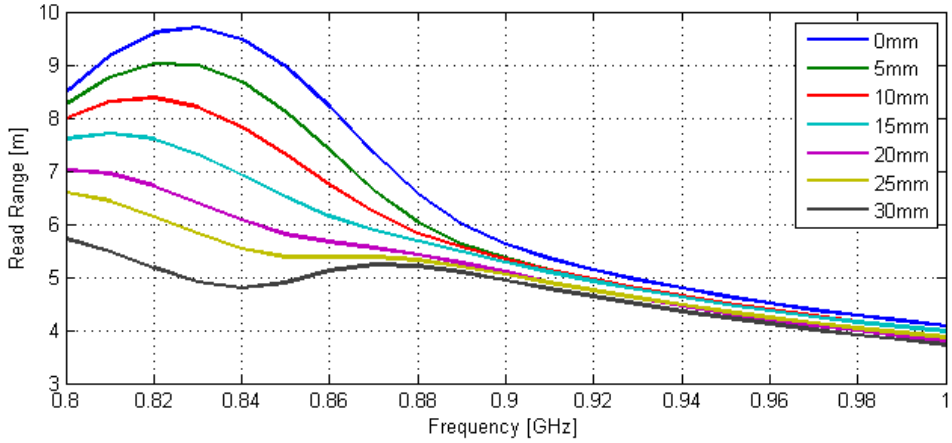

(b) Read ranges of the reference tag

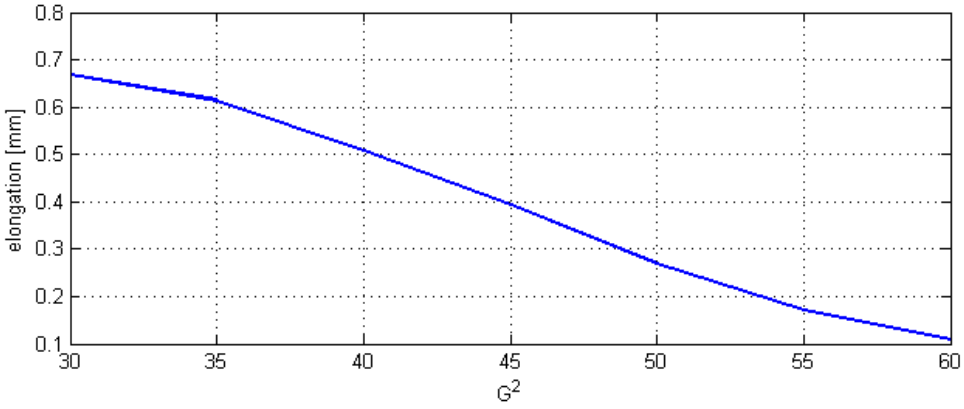

(c) G^2 of the reference tag

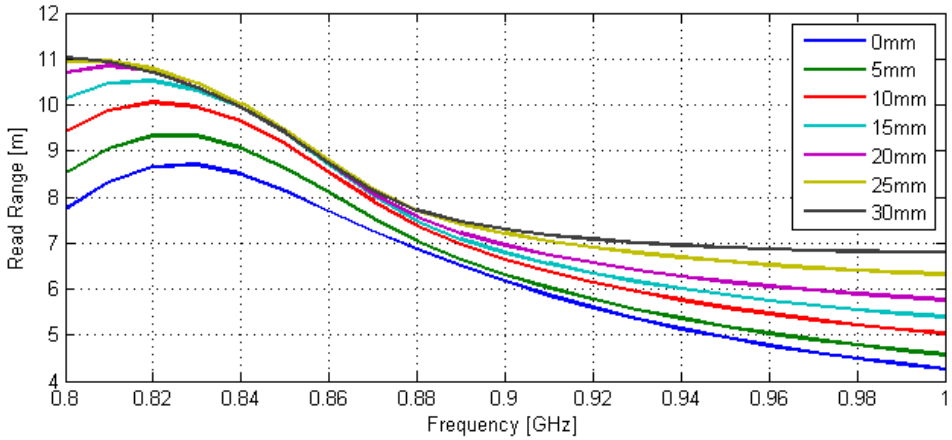

(d)Read ranges of sensor tag

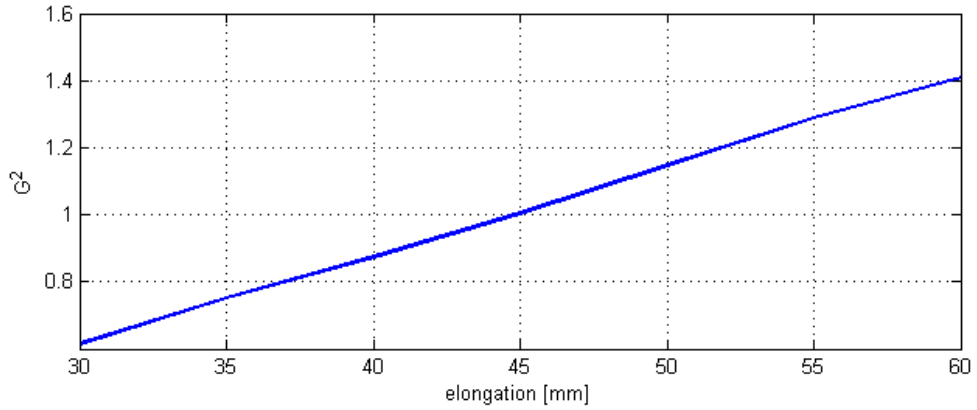

(e) G^2 of sensor tag

Figure 27. *The simulation result of linear configuration model.*

In the linear configuration model, the read range of the reference tag, around 11.5 m, is higher than the sensor tag which has the read ranges from 9.5 m ~ 11.5 m. The G^2 of both the reference tag and the sensor tag meet the requirements. Thus, this configuration is also a candidate for the strain sensor system.

The last configuration is the orthogonal configuration as shown in Figure 28. The size parameters are different from the previous configuration to minimum the influence of coupling at the target frequency 866 MHz. The simulation results are shown below.

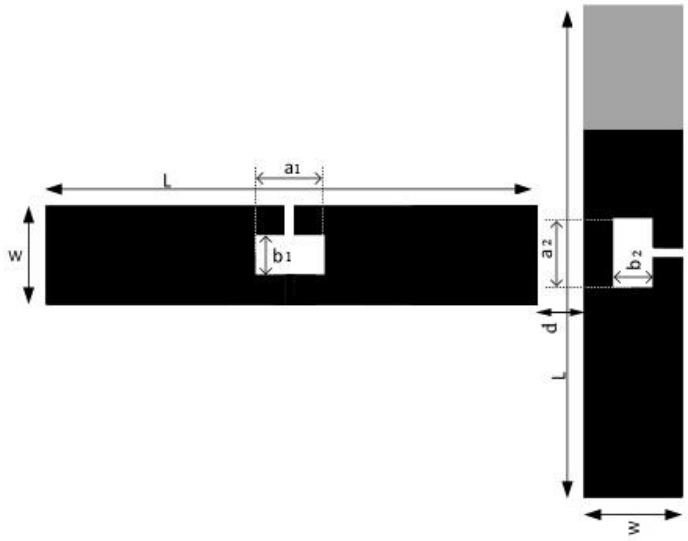

a1	b1	a2	b2	L	W	d
17.3mm	10mm	17.3mm	10mm	100mm	20m	5m

(a) The orthogonal configuration

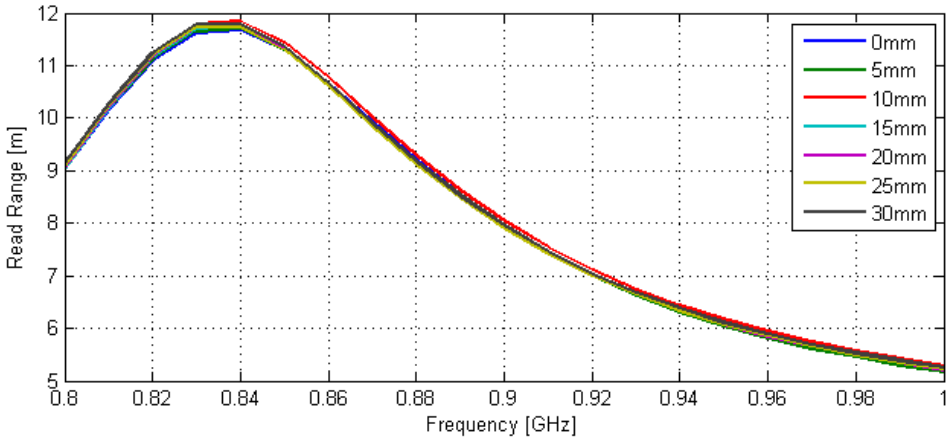

(b) Read ranges of the reference tag

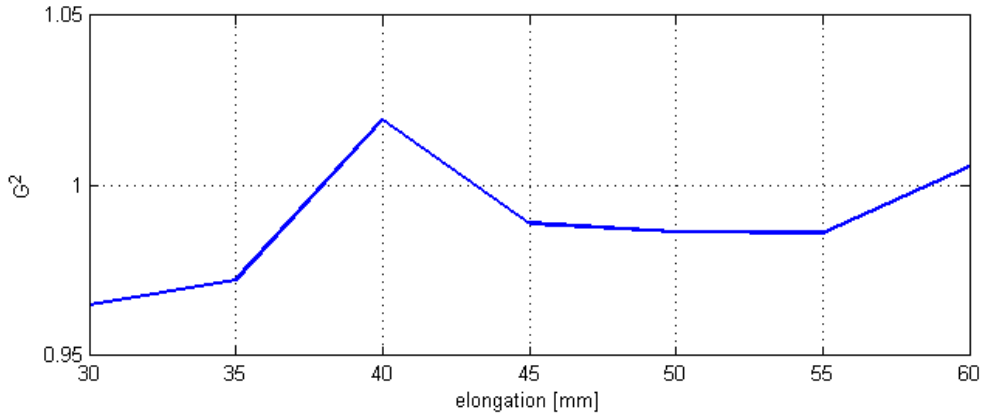

(c) G^2 of the reference tag

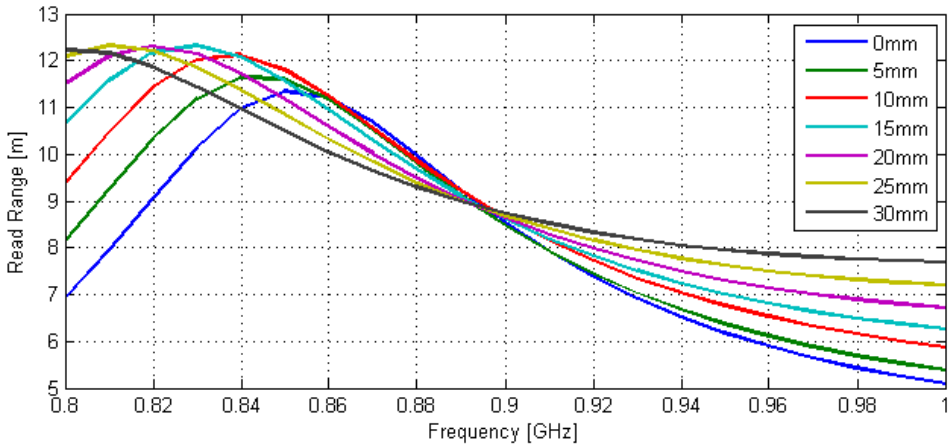

(d) Read ranges of sensor tag

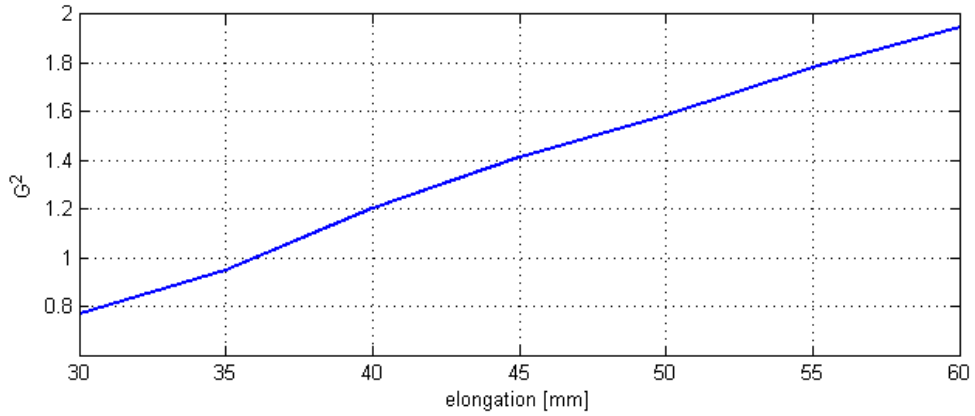

(e) G^2 of sensor tag

Figure 28. *The simulation result of orthogonal configuration model.*

Utilizing the orthogonal configuration, the read ranges of the reference tag with different elongations are very similar at the whole frequency band especially at 866 MHz. The read ranges of the sensor change the same distance at each 5 mm elongation.

The G^2 of the reference tag changes only 0.03 dB when the sensor is straining. For the sensor tag, the G^2 is linear with the elongation.

In the parallel configuration model and linear configuration model, the distance *d* between tags influence the results significantly. With larger *d*, the read range of the reference tag is more constant when different elongations are applied. As for orthogonal configuration model, the sensor tag and the reference tag have different polarization. Thus the coupling between them has the minimum value regardless the distance between the tags.

4.3 Measurement in Chamber

In this part, I use Tagformance to test the read ranges and backscattered power of the hand-made tags. The step size of the frequency sweep in Tagformance is 1 MHz and all the tags are tested with the wake-up power of the IC. By comparing the read ranges of the simulation and measurement I can realize whether my simulation matching the measurement results or not. The backscattered power is the most vital parameter in my test. In the practical case. The reference tag is utilized to characterize the channel feature. Thus, after eliminating the influence of the channel, the variation of the backscattered power of the sensor is caused by the strain. Thus, we define the variation ΔP as:

$$\Delta P[\mathrm{dB}] = P_{sensor}[\mathrm{dBm}] - P_{reference}[\mathrm{dBm}], \tag{4.9}$$

ΔP should change linearly with the strain to indicate the elongation of the sensor. P_{sensor} is the backscattered power of the sensor tag unit in dBm, $P_{reference}$ is the backscattered power of the reference tag unit in dBm.

- Parallel tags

The layout of parallel tags and test results of the parallel configuration model as shown in Figure 29.

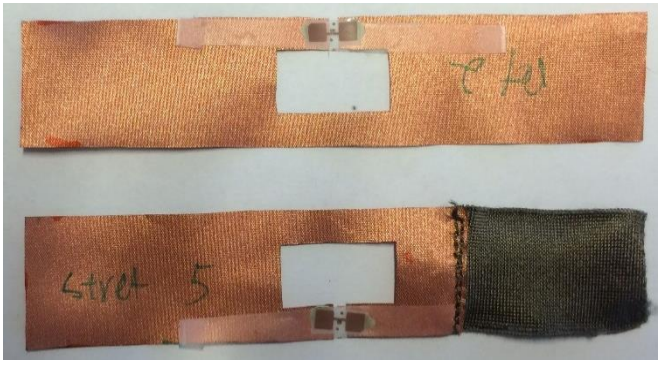

(a) Parallel tags

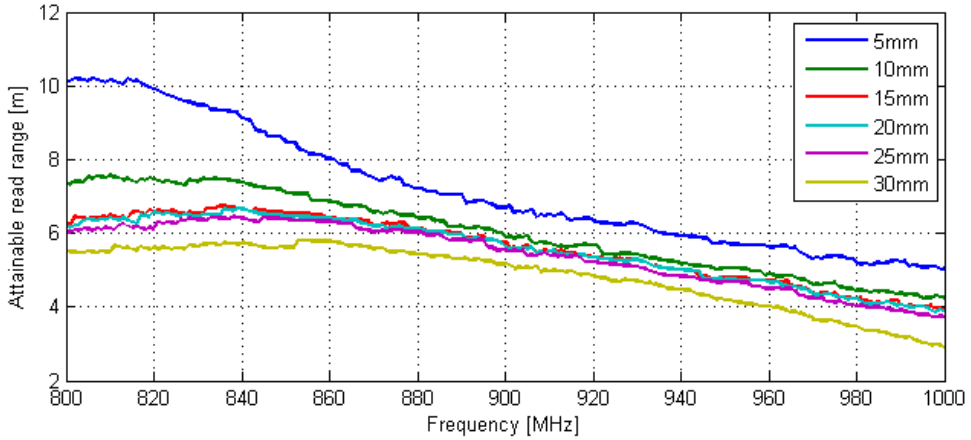

(b) Read ranges of Sensor tag

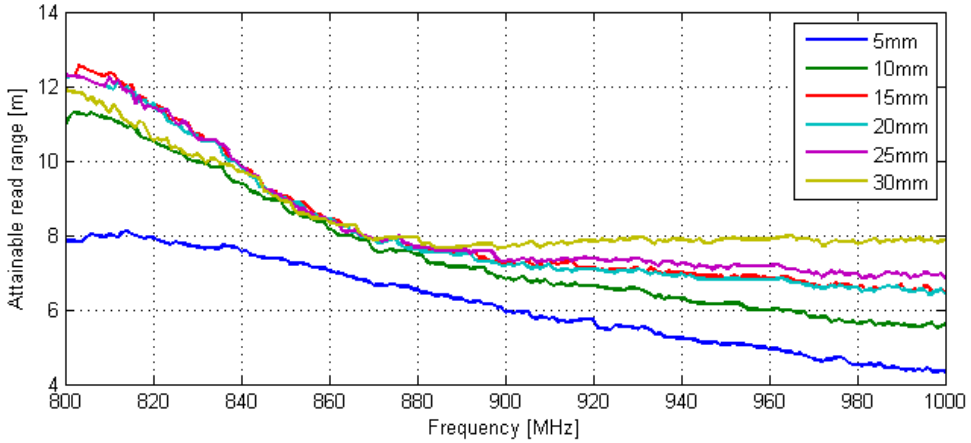

(c) Read ranges of reference tag

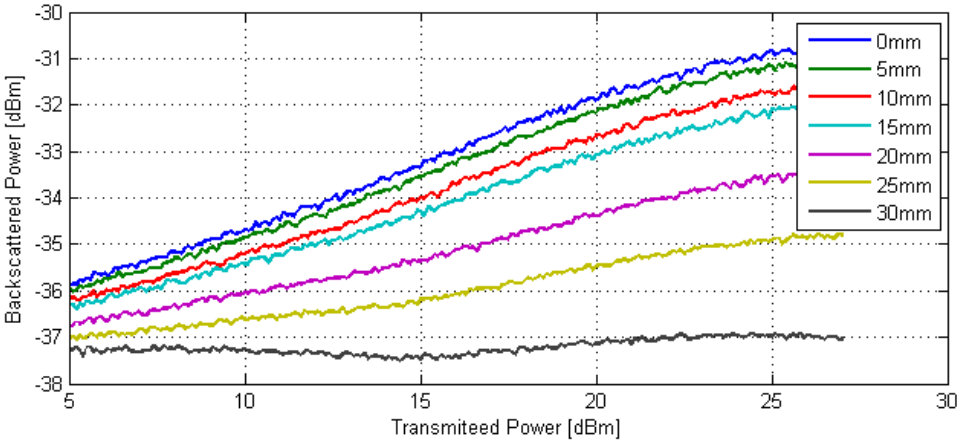

(d) Backscattered power of the reference tag

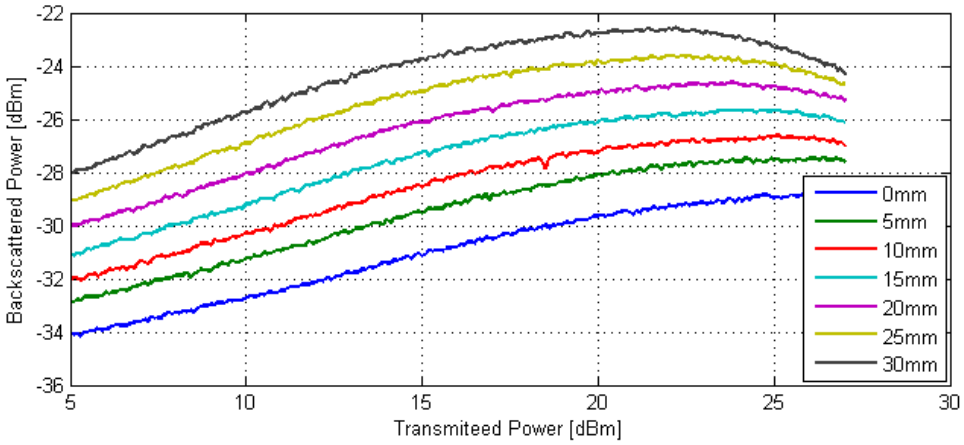

(e) Backscattered power of the sensor tag

Figure 29. *The test result of parallel tags in chamber.*

As seen in Figure 29, the backscattered power of the sensor has an equal variation with the same elongation length. However, for the reference tag, the backscattered power changes a lot at different elongation, especially when transmitted power is higher. In this case, this configuration is not an appropriate configuration for the strain sensor.

- Linear tags

In this test, the distance between tags is 20 mm to provide sufficiently small coupling the coupling. The configuration model and test results are illustrated in Figure 30.

(a) Linear tags

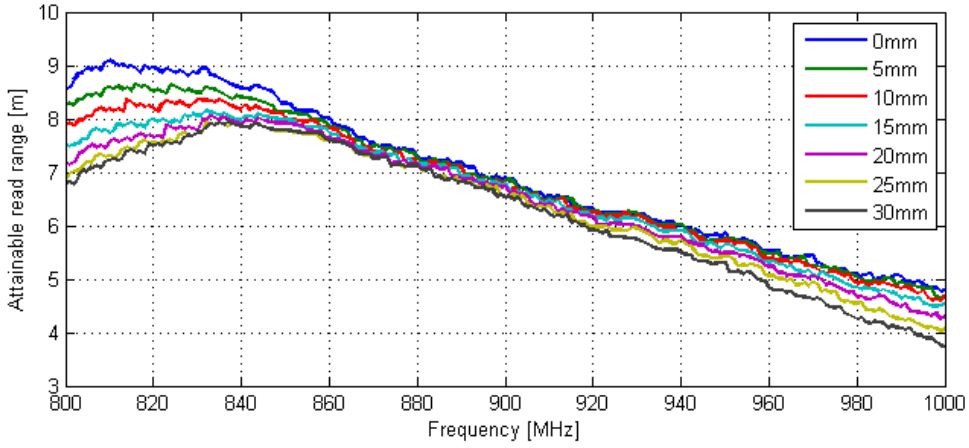

(b) Read ranges of the reference tag

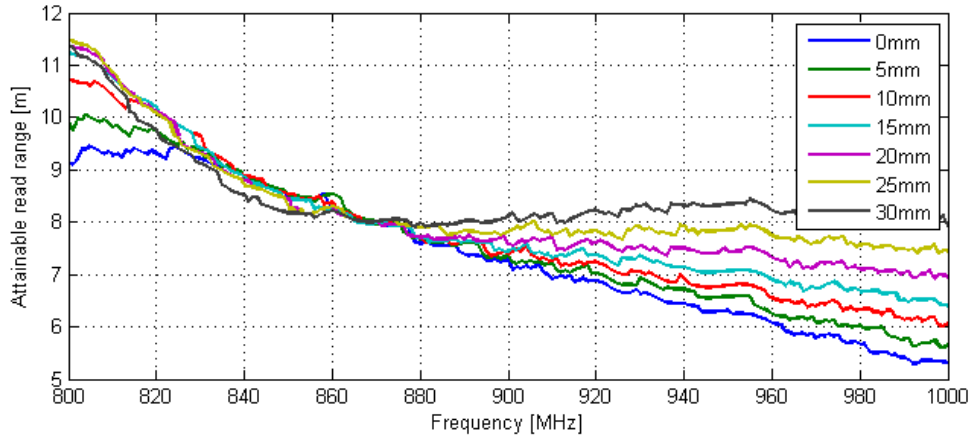

(c) Read ranges of the sensor tag

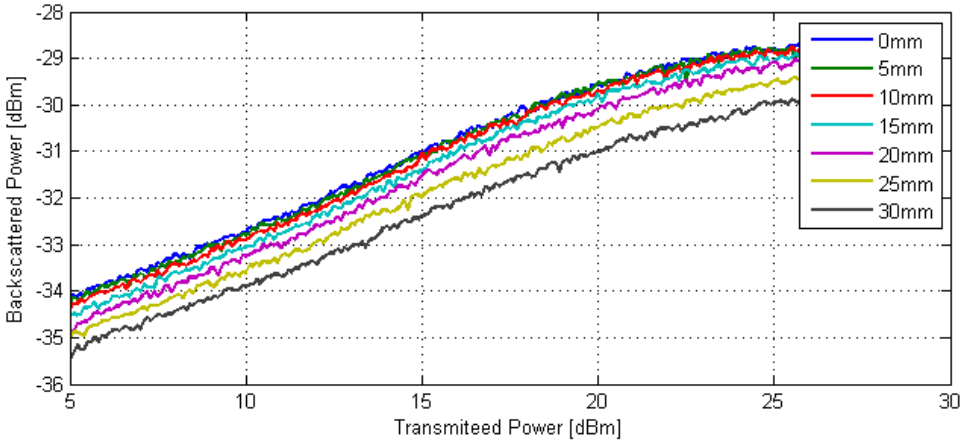

(d) Backscattered power of the reference tag

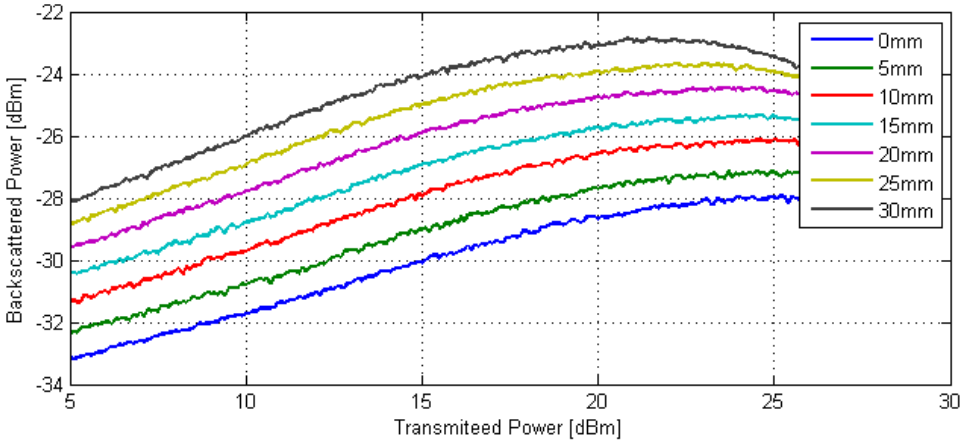

(e) Backscattered power of the sensor tag

Figure 30. *The test result of linear tags in chamber.*

In this configuration model, with the different elongations, the read ranges of the reference tag at the target frequency band are similar. The backscattered power variation of the reference tag is small at different elongations and different reader transmitted power. In addition, for the sensor tag, the backscattered power increases with the strain uniformly. Thus, these test results meet the basic requirements of the strain sensor tag system.

As shown in Figure 31, the relationship of elongation and ΔP ($P_{sensor} - P_{reference}$.) is studied to check if the backscattered power is proportional to the elongation without the influence of the channel. The test is made at 864 MHz ~ 867 MHz and the transmitted power is the threshold power of the sensor tag. Based on the figure, the parameter ΔP rises linearly with the elongation. This means, by monitoring the backscattered power at the reader end, we can estimate the elongation of the sensor in the rough.

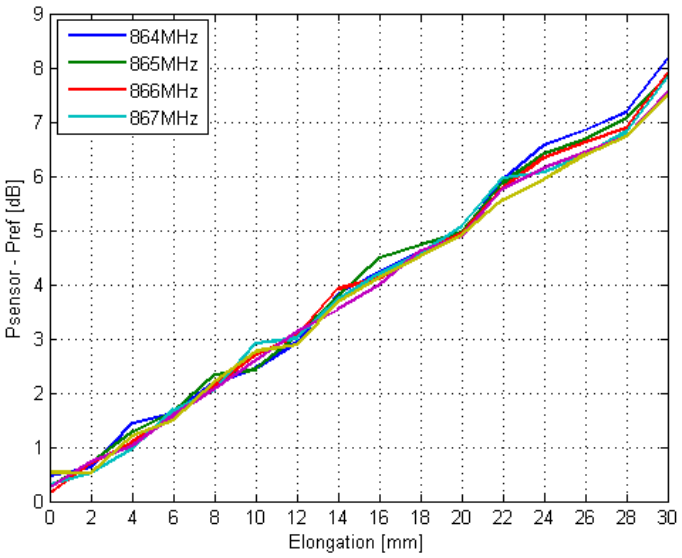

Figure 31. *The difference of the backscattered power between the sensor tag and reference tag.*

In the practical case, the transmitted power of the reader always higher than the threshold power of the sensor tags. Thus, it is also important to test the backscattered power at another fix-transmitted power and find the relation between the backscattered power and the elongation. Then we use 10 dBm transmitted power and 866 MHz signal frequency to measure then sensor tag at 0 ~ 30 mm elongation. The result is shown in Figure 32.

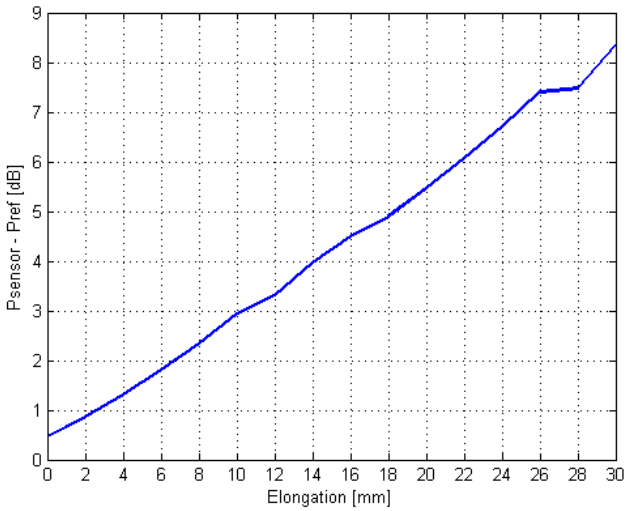

Figure 32. *The difference of the backscattered power at 10 dBm transmitted power.*

In Figure 32. ΔP is also proportional to the elongation. Thus, we can consider that ΔP is linearly related to the elongation at a broad transmitted power band at the frequency 866 MHz.

- Orthogonal tags

The configuration and test results are shown in Figure 33.

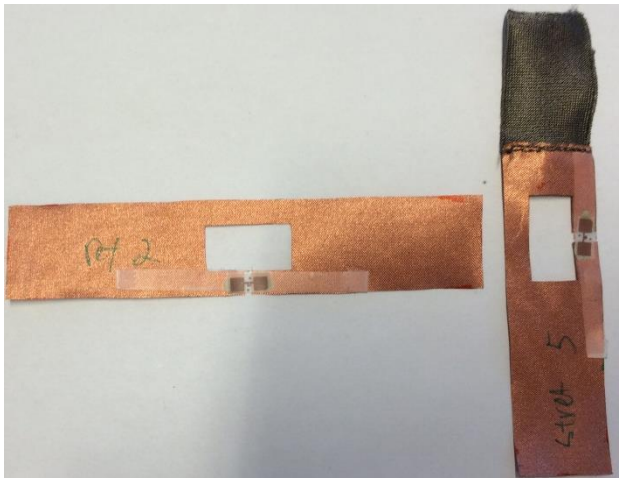

(a) Orthogonal tags

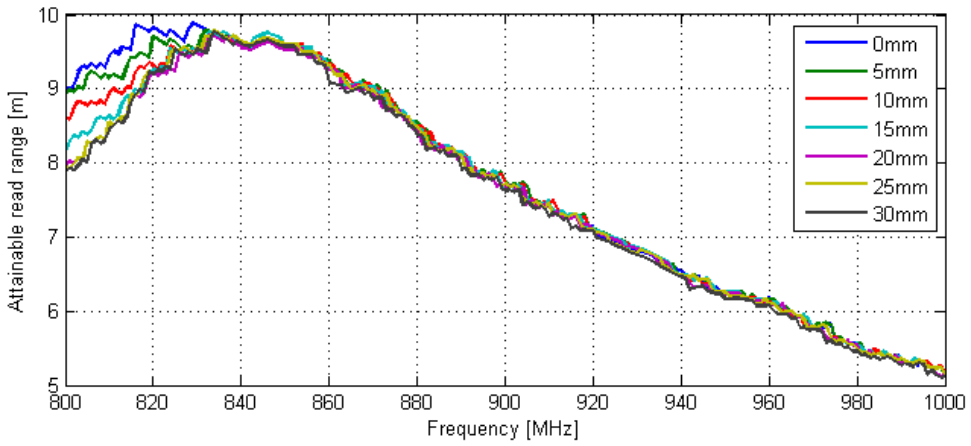

(b)Read ranges of the reference tag

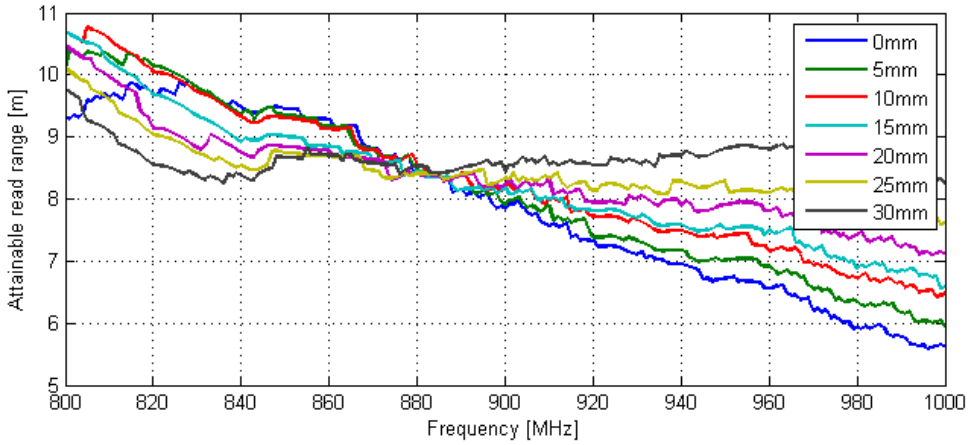

(c) Read ranges of the sensor tag

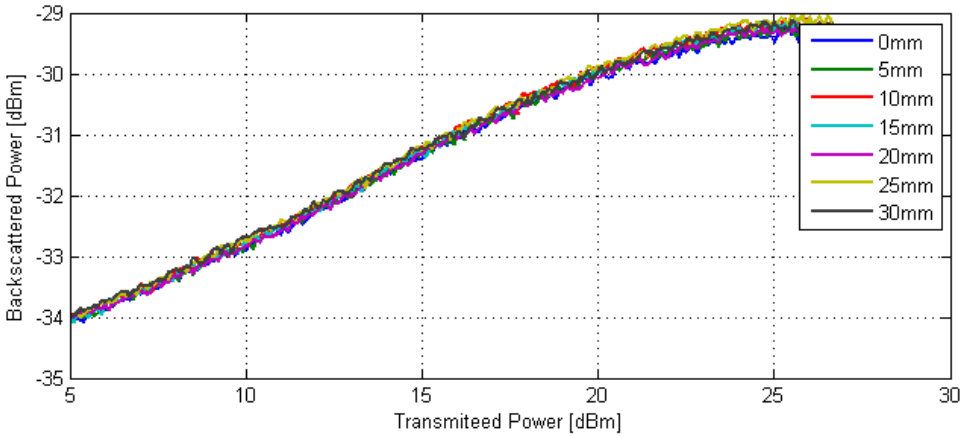

(d)Backscattered power of the reference tag

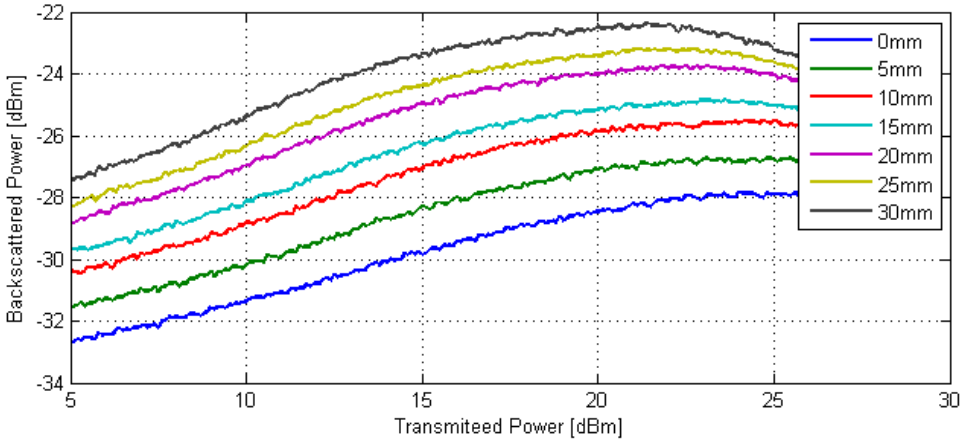

(e) Backscattered power of the sensor tag

Figure 33. *The test result of orthogonal tags in chamber.*

In the orthogonal configuration model, the read ranges and the backscattered power are highly constant with the stretch of the sensor at the target bandwidth. It indicates that this configuration can minimize the coupling between the tags among the studied configurations. The backscattered power of the sensor tag changes regularly with the stretch. Thus, we can speculate that in this configuration model, ΔP has linear relationship with the elongation. Then, we test the relationship between ΔP and elongation using the threshold power of the sensor at 864 MHz ~ 868MHz. The step size of the elongation is 2 mm. The measurement results are shown in Figure 34.

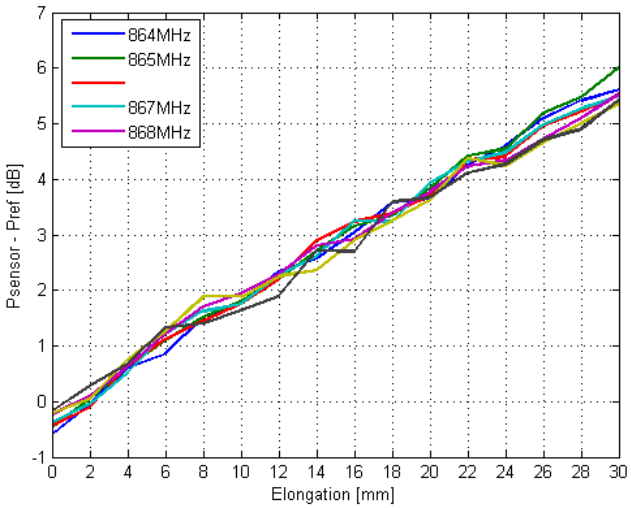

Figure 34. *The difference of the backscattered power between the sensor tag and reference tag.*

In Figure 34. ΔP is nearly proportional to the sensor strain. In other words, ΔP changes regularly when we stretch the sensor by the same step size. Thus this model can also be used for monitor the elongation of the sensor tag by calculating ΔP using the value of

the backscattered power at the reader end with the threshold transmitted power. The longest stretchable length is 30 mm.

Then we check the relationship between the ΔP and sensor elongation at 10 dBm transmitted power to see if this configuration model can be used in other transmitted power more highly than the threshold power. The step size of the strain is 2 mm and the maximum elongation is 30 mm.

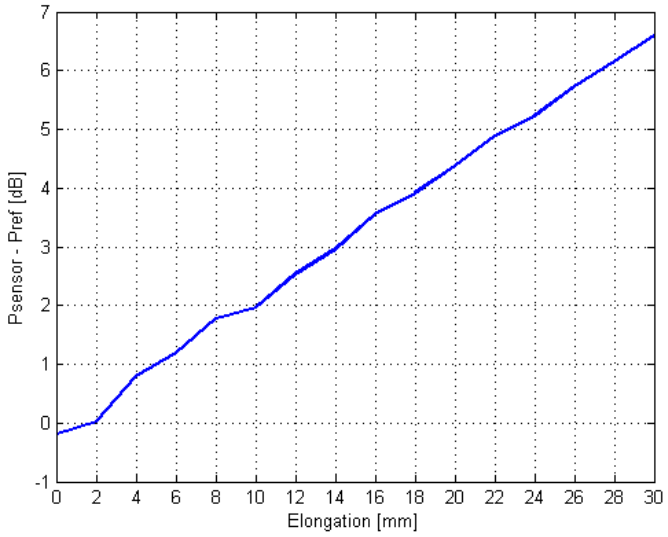

Figure 35. *The difference of the backscattered power at 10 dBm transmitted power.*

Figure 35. shows that the ΔP is almost linear to the sensor elongation when transmitted power is not the threshold power of the IC. Thus the orthogonal tags also meet the basic requirements of the textile wireless RFID sensor tag system.

By measuring the different configuration models in the chamber, we find that the parallel configuration does not adapt to making the RFID strain sensor system. The linear configuration and parallel configuration perform better in the measurement. They both meet the basic requirements of sensor tag systems. Thus in next step, we only measure these two models in the real environment.

4.4 Practical Environment Measurement

In this step, we measure these models in four practical conditions as shown in Figure 36. with fixed 28.4 dBm transmitted power simultaneously. The reader is circular polarization, which introduces around 30% polarization power loss compared to the power in the communication with the linear polarized tags. The tags will be measured in the line-of-sight condition. We record the backscattered power of the reference tag and the sensor tag at same time, which is received at the reader end, to study the law of the

backscattered power variation with different elongation of the sensor. The step size for the strain is 5 mm and the total extension length is 30 mm.

Condition 1: in a narrow channel between two walls.

Condition 2: in an open-air condition, tags face to the reader

Condition 3: in an open-air condition, tags have a tilt to the reader

Condition 4: in an open-air condition, tags located in the side of the reader.

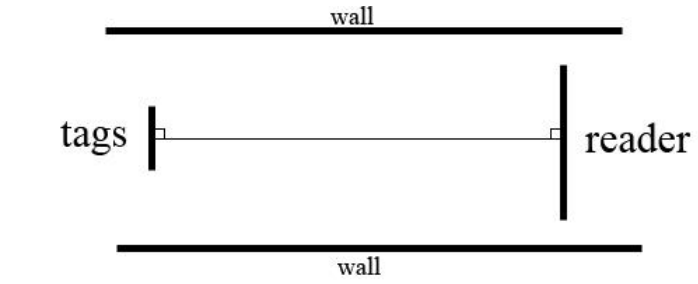

(a) Condition 1

(b) Condition 2

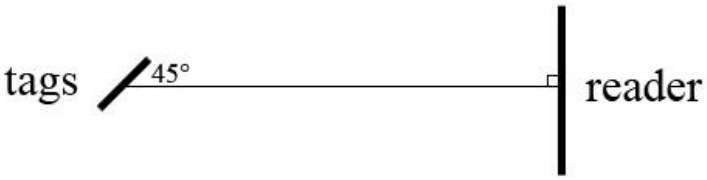

(c) Condition 3

(d) Condition 4

Figure 36. *Measurement conditions.*

- Linear tags

The measurement results of the linear tags in the four different conditions are shown in Figure 37.

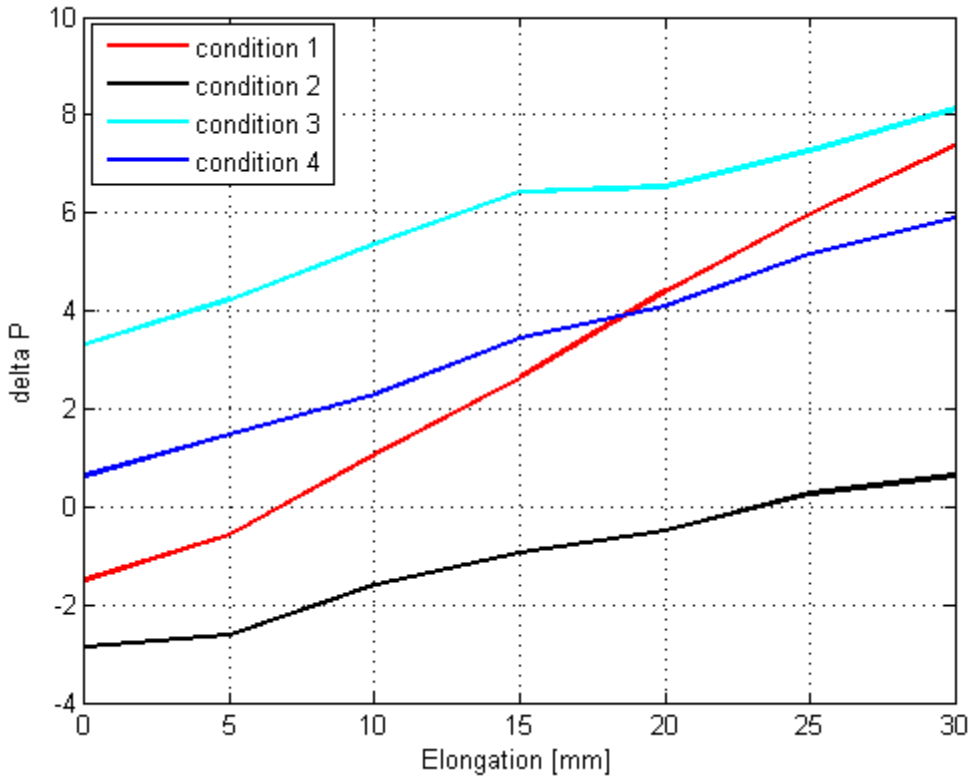

Figure 37. *The test result in different condition of linear tags.*

The read ranges of tags in different conditions are about 1.5 m, 6 m, 6 m, 3 m respectively. So we measure the tags at 1 m, 3 m, 3 m, 2.5 m with the fixed transmitted power 28.4 dBm. As seen in Figure 37, ΔP increases with the stretch and almost proportional to the elongation in all conditions. However, with the sensor stretching, the ascending speed of ΔP is different in each condition. The condition 1 has the fastest ascending speed started at -1.8 dB and condition 2 has the slowest speed. ΔP also have different start point in different condition. By comparing condition 2 to condition 3, we can find that the polarization of the tag can affect the measurement result. Besides, in the practical test, the tags will loss connection with the reader when they turn around more than 60°. The difference of tags' reader ranges of condition 2 and condition 4 indicates that the read range of the tag sensor system also depends on the radiation pattern of the reader. By locating the tags by the side of the reader, the value of ΔP will increase.

- Orthogonal tags

The measurement results of the orthogonal tags in the four different conditions are shown in Figure 38.

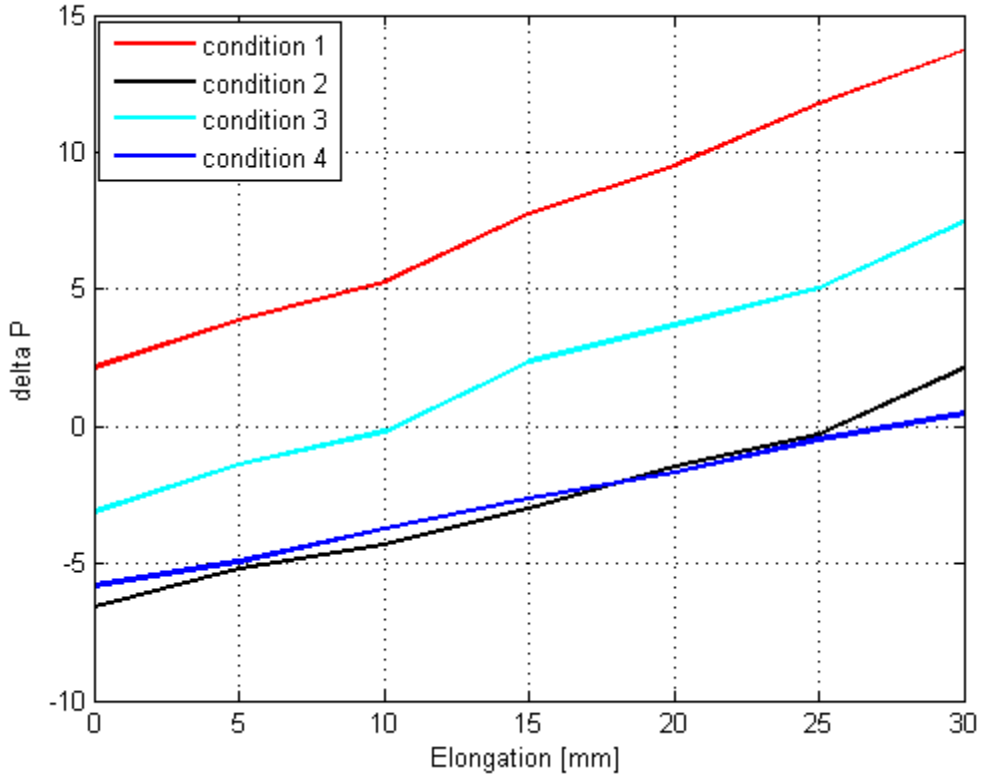

Figure 38. *The test result in different condition of orthogonal tags.*

In these four conditions, the parameter ΔP is increasing with the elongation and always proportional to the sensor elongation. The lines in the Figure 38 are more linear than in the linear configuration model, which means the orthogonal tags perform better than the linear tags in reducing the coupling between the nearby tags. The read ranges of different conditions of this model are almost the same with the linear configuration model in practical. Thus we test the tags at the same distance in this case. Condition 1 has the largest slope of the line and condition 4 has the smallest one. The differences of the slope of ΔP in different conditions are smaller than in linear model. It means the influence caused by the polarization is smaller than linear model in the orthogonal tags model.

5. CONCLUSIONS

This thesis involved the testing and development of the wireless strain sensor RFID tags. To make the sensor working without the influence of the channel, the characters of the channel need to be revealed. Thus, a reference tag is placed closely to the sensor tag to characterize the channel parameters. The coupling effect may appear between the nearby antennas as well. It can be reduced by designing the parameters of antennas size and antennas' configuration. Three different antenna configurations are designed with the particular antenna parameters to achieve the goal. In addition, the designed antennas are measured in the practical case for checking the performance and other influence factor of strain sensor system.

By the simulation and chamber test, three different antenna configuration models were tested to decrease the coupling. The parallel configuration model performed badly in the chamber test. The backscattered power of reference tag changed a lot with the higher transmitted power at different elongation. As for linear configuration model, the difference of backscattered power between the reference tag and sensor tag (ΔP) was proportional to the sensor elongation, which meant the elongation of the sensor could be read at the reader end approximately. However, the polarization of the tag and reader can influent the measurement results in this model. The orthogonal configuration model performed better in both simulation and practical test. Furthermore, the linearity of the elongation and the power difference ΔP is better in this case. However, this configuration occupies larger area.

In the future research, the textile wireless strain sensor can still be improved in various aspects, such as improving the stability of the system, reducing the size of the sensor, increasing the read range, and reducing the influence of polarization. During this work, it was found that the stretchable part of the tag is hard to restore after the long-time stretching. Thus, new material of the stretchable part can be studied to improve the performance. In addition, more configuration models will be studied to minimize the coupling influence.

REFERENCES

[1] Klaus Finkenzeller, “RFID Handbook” 2nd edition, 2003

[2] V. Daniel Hunt, Albert Puglia, Mike Puglia, “RFID: A Guide to Radio Frequency Identification”, 2007

[3] D. M. Dobkin, The RF in RFID, Passive UHF RFID in Practice, Elsevier Inc., United States of America, 2008.

[4] Feiyuan Long *et al.*, "Implementation and wireless readout of passive UHF RFID strain sensor tags based on electro-textile antennas," *2015 9th European Conference on Antennas and Propagation (EuCAP)*, Lisbon, 2015, pp. 1-5.

[5] S. Manzari, T. Musa, M. Randazzo, Z. Rinaldi, G. Marrocco, “A passive temperature radio sensor for concrete maturation monitoring,” in Dig. IEEE RFID-TA Conf., 8-9 Sep., 2014, pp. 121-126

[6] C. Occhiuzzi, A. Rida, G. Marrocco, M. M. Tentzeris, “RFID passive gas sensor integrating carbon nanotubes,” IEEE Trans. Microw. Theory Techn., vol. 59, no 10., Oct. 2011, pp. 2674-2684.

[7] J. Virtanen, L. Ukkonen, T. Björninen, A. Z. Elsherbeni, L. Sydänheimo, “Inkjet-printed humidty sensor for passive UHF RFID systems,” IEEE Trans. Instrum. Meas., vo. 60, no. 8, Aug. 2011, pp. 2768-2777.

[8] A. A. Babar, S. Manzari, L. Sydänheimo, A. Z. Elsherbeni, L. Ukkonen, “Passive UHF RFID tag for heat sensing applications,” IEEE Trans. Antennas Propag., vol. 60, no. 9, Sep. 2012, pp. 4056-4064.

[9] Per-Simon Kildal, “Foundations of Antenna Engineering”, 2015

[10] Constantine A. Balanis, “Antenna Theory: Analysis and Design, 3rd Edition”, May 2005

[11] Warren L. Stutzman, Gray A. Thiele, “Antenna theory and design” 2nd Edition, 1998

[12] S. A. Schelkunoff, H. T. Friis, “Antennas: Theory and Practice”, 1952, p.127

[13] Constantine A. Balanis: “Antenna Theory, Analysis and Design”, John Wiley & Sons, Inc., 2nd ed. 1982

[14] Robert s. Elliott, “Antenna Theory and Design: Revised Edition”, 2003

[15] "Dipole Antenna / Aerial tutorial". Resources. Radio-Electronics.com, Adrio Communications, Ltd. 2011. Retrieved April 29, 2013.

[16] A. Brogdon, “Low Profile Amateur Radio”, 2006

[17] Narayan, C.P., “Antennas and Propagation”. Technical Publications. 2007

[18] Bakshi K.A., A.V.Bakshi, U.A.Bakshi, “Antennas And Wave Propagation”, Technical Publications, p. 1.17, 2009

[19] Peter Joseph Bevelacqua, ‘Antenna-Theory’ [http://www.antenna-theory.com/]

[20] Simonr Saunders, Alejandro Aragón-Zavala, “Antennas and Propagation for Wireless Communication Systems 2nd Ed”, 2007

[21] Theodore S. Rappaport, “Wireless Communications: Principles and Practice” 2nd Edition, 2002

[22] Ahlin, L., J. Zander. "Principles of wireless communications, Student literature." Massachusetts Insititute of Technology, 1998

[23] Sandib Lahiri, “RFID Sourcebook” , IBM Press, 2006

[24] Jim Pomager, “Q&A With Zoltan Cendes, Founder, Chairman, And CTO Of Ansoft Corporation”, Editor in Chief, RF Global Net

[25] Baidu, “Baidu cyclopedia: HFSS”, [http://baike.baidu.com/link?url=AubLahrUtGF7TNEZPY2ZHI1zMPzNBi8vOyoP1GB6t9II_NW0HvYp0cTXkwtD8JGjo0O99qgo9cisWTEsRQwDPq]

[26] J. Virkki, T. Björninen, S. Merilampi, L. Sydänheimo, L. Ukkonen,”The effects of recurrent stretching on the performance of electro-textile and screen-printed ultra-high-frequency radio-frequency identification tags”, published online ahead of print in Text. Res. J., Aug. 2014, 9 p.

[27] “Poynting vector, radiated power, radiation resistance”, [http://jsa.ece.illinois.edu/hcmut/ece350/notes/9.pdf]

[28] David M. Pozar , “Microwave Engineering”, Wiley, 2004.